Tridentate Complexes of Group 10 Bearing Bis-Aryloxide N-Heterocyclic Carbene Ligands: Synthesis, Structural, Spectroscopic, and Computational Characterization

ARTICLE *in* ORGANOMETALLICS · MARCH 2014

Impact Factor: 4.13 · DOI: 10.1021/om5003446

6 AUTHORS, INCLUDING:

Etienne Borre
University of Strasbourg
17 PUBLICATIONS **118** CITATIONS
SEE PROFILE

Georges Dahm
Laboratoire National de Santé
10 PUBLICATIONS **61** CITATIONS
SEE PROFILE

Matteo Mauro
University of Strasbourg
38 PUBLICATIONS **525** CITATIONS
SEE PROFILE

Samuel Dagorne
French National Centre for Scientific Research
85 PUBLICATIONS **1,569** CITATIONS
SEE PROFILE

ORGANOMETALLICS

Article

pubs.acs.org/Organometallics

Tridentate Complexes of Group 10 Bearing Bis-Aryloxide N-Heterocyclic Carbene Ligands: Synthesis, Structural, Spectroscopic, and Computational Characterization

Etienne Borré,[†] Georges Dahm,[†] Alessandro Aliprandi,[‡] Matteo Mauro,*[,‡,§] Samuel Dagorne,*[,∥] and Stéphane Bellemin-Laponnaz*[,†,§]

[†]Institut de Physique et Chimie des Matériaux de Strasbourg, Université de Strasbourg CNRS UMR 7504, 23 rue du Loess, BP 43, F-67034 Strasbourg Cedex 2, France

[‡]Laboratoire de Chimie et des Biomatériaux Supramoléculaires, Institut de Science et d'Ingénierie Supramoléculaires (ISIS), Université de Strasbourg UMR 7006, 8 allée Gaspard Monge, F-67083 Strasbourg, France

[§]University of Strasbourg Institute for Advanced Study (USIAS), 5 allée du Général Rouvillois, 67083 Strasbourg, France

[∥]Institut de Chimie de Strasbourg, CNRS-Université de Strasbourg UMR 7177, 1 rue Blaise Pascal, F-67000 Strasbourg, France

Supporting Information

ABSTRACT: A series of group 10 complexes featuring chelating tridentate bis-aryloxide N-heterocyclic carbenes were synthesized and characterized by using different techniques. Ni(II), Pd(II), and Pt(II) complexes were isolated in good yields by straightforward direct metalation of the corresponding benzimidazolium or imidazolium precursors in a one-pot procedure. All of the compounds were fully characterized, including single-crystal X-ray diffractometric determination for three of the derivatives. In the solid state, the complexes adopt a typical square-planar coordination geometry around the platinum atom, sizably distorted in order to comply with the geometrical constraints imposed by the bis-aryloxide N-heterocyclic carbene ligand. For platinum and palladium derivatives, a joint experimental and theoretical characterization was performed in order to study the optical properties of the newly prepared complexes by means of electronic absorption and steady-state and time-resolved photophysical techniques as well as density functional theory (DFT) and time-dependent DFT in both vacuum and solvent. When the temperature was lowered to 77 K in frozen glassy matrix, three platinum complexes showed broad and featureless, yet weak, photoluminescence in the green region of the visible spectrum with excited-state lifetimes on the order of a few microseconds. On the basis of joint experimental and computational findings and literature on platinum complexes, such emission was assigned to a triplet-manifold metal−ligand-to-ligand charge transfer (^{3}MLLCT) transition.

INTRODUCTION

N-heterocyclic carbene chemistry (NHC) has become a very prolific field of research over the past 15 years.[1,2] Due to their unique steric and electronic properties, NHCs have emerged as a powerful class of ligands in organometallic chemistry and homogeneous catalysis.[3] Interestingly, the applications of metal NHC complexes in other fields remain much less studied, although some advances have emerged these past few years.[4] Very promising results have in particular been reported in biology, such as anticancer and antimicrobial agents[5] and bioimaging,[6] as well as in materials chemistry for the preparation of liquid crystals,[7] low-molecular-weight gelating materials,[8] and luminescent derivatives.[9]

Group 10 complexes containing N-heterocyclic carbene ligands are well-established catalysts in a variety of transformations, including cross-coupling, cycloisomerization, polymerization, and hydrosilylation reactions.[10] Furthermore, group 10 transition metals bearing NHC-based ligands have shown attractive properties for use in materials science as, for instance, luminescent complexes[9] and may also be of interest for biomedical applications.[5,9,11]

Over the past few years π-conjugated cyclometalating ligands containing NHC moieties have increasingly been studied for the preparation of transition-metal complexes exerting a sizable spin−orbit coupling effect (SOC), such as those of Ir(III) and Pt(II), suitable for the preparation of phosphorescent triplet emitters.[12] After seminal studies by Baldo, Thompson, and Forrest over a decade ago,[13] cyclometalated platinum(II) species and numerous iridium(III) complexes were reported to exhibit photoluminescence quantum yield (PLQY) in some cases approaching 100%.[14] In addition, the ability of phosphorescent complexes to act as electro-active phosphors in optoelectronics devices, such as organic light emitting diodes (OLEDs) and light emitting electrochemical cells (LEECs) has been widely demonstrated.[12b−e,14d−g,15]

Received: March 31, 2014

   dx.doi.org/10.1021/om5003446 | *Organometallics* XXXX, XXX, XXX−XXX

Chart 1

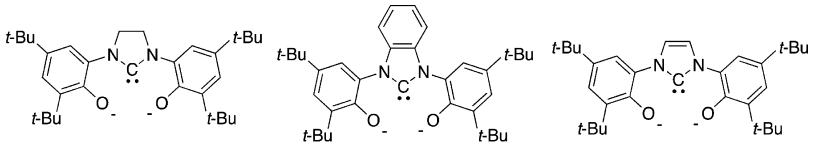

In this area, NHC-based supporting ligands currently play a pivotal role due to their attractive electronic properties such as (i) the formation of strong M−C_{NHC} coordination bonds, (ii) strong σ-donation to the metal center, allowing the typically quenching d−d metal-centered (MC) states to rise up in energy and thus reduce the nonradiative deactivation pathways, and (iii) high-energy π^* orbitals mostly due to the weak π-accepting ability, which allows the emissive excited state to lie in higher energy regions, in particular in the blue to ultraviolet (UV) portion of the electromagnetic spectrum.[12c−e,16]

The molecular rigidity of the emitter, of crucial importance to access robust phosphorescent complexes suitable for optoelectronics applications, disfavors nonradiative deactivation channels by means of, for instance, geometrical distortions.[17] One of the most successful ways to increase molecular rigidity lies in the use of chelating ligands with higher denticity.[12c−e,18] Improvements of photoluminescence quantum yield (PLQY), (photo)stability, and color tuning in platinum(II)-based complexes bearing NHC-containing tridentate[14e−h] and tetradentate[12c,14f,19] chromophoric ligands have been reported, showing electronic transitions with admixed ligand-centered (LC) $\pi-\pi^*$ and metal-to-ligand charge transfer (MLCT) character.

It is worth noting that square-planar Pt(II) and Pd(II) complexes typically exhibit a high tendency toward stacking when in the solid phase or when embedded in matrices, thus reducing their solubility and solution processability. In the case of luminescent derivatives, such a tendency often results in a loss of emission color purity and poorer PLQY, mostly due to aggregation quenching phenomena and formation of excimers[20] or lower-energy excited states with triplet metal−metal-to-ligand charge transfer (^{3}MMCT) character upon establishment of closed-shell metallophilic interactions.[21] Nevertheless, enhancement of the photophysical properties upon aggregation are sometimes observed.[22] To overcome detrimental aggregation, bulky substituents such as *tert*-butyl and adamantyl groups are typically introduced on the ligand backbone.[15f,23]

Seeking for robust NHC-incorporating pincer-type chelating ligands, we developed a straightforward synthesis of the new family of tridentate type bis-aryloxide-NHC ligands **A** (Chart 1), a ligand structure well suited for coordination to V(V), Mn(III), and group 4 and 13 metals (Ti, Zr, Hf, Al).[24] The coordination of such structures to late-transition-metal centers has been little explored, prompting us to investigate the coordination chemistry of the tridentate bis-aryloxide-NHC ligand with group 10 transition metals.[25] It was envisioned that the introduction of a benzimidazol-2-ylidene core into the structure (**B**) might result in a π-conjugated system over the three six-membered rings able to accommodate heavy-metal centers. The resulting transition-metal complexes may display interesting photophysical properties.

Herein we report on the straightforward and high-yield synthesis of robust NHC-group 10 complexes supported either by ligand **B** or the novel and presently described imidazolidene ligand **C**. The photophysical properties of some of the platinum complexes were also studied both in solution at room temperature and in glassy matrix at 77 K.

RESULTS AND DISCUSSION

Synthesis and Structural Characterization of Ni, Pd, and Pt Complexes. The benzimidazolium precursor **1** was prepared according to our previous report.[26] The azolium salt precursor was thus treated with 1 equiv of MCl_2 (M = Ni, Pd, Pt) and an excess of potassium carbonate in pyridine at 100 °C for 12 h (Scheme 1).[27] Analysis of the crude product by ^{1}H

Scheme 1. Synthesis of Group 10 Complexes 2

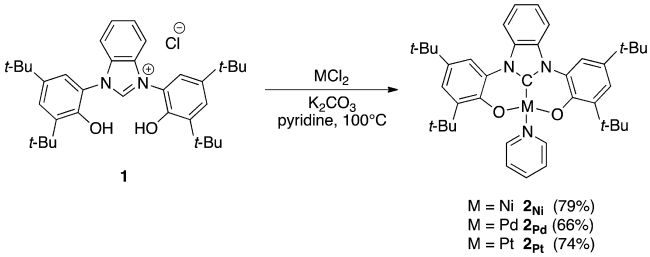

NMR spectroscopy confirmed the absence of any residual azolium and phenol moieties. Purification of the complexes by flash column chromatography afforded the corresponding nickel, palladium, and platinum complexes (NHC)M(pyridine) ($\mathbf{2_{Ni}}$, $\mathbf{2_{Pd}}$, and $\mathbf{2_{Pt}}$, respectively) in 66−79% yield. The proposed formulations were confirmed by mass spectrometry and elemental analysis. The formation of the carbene complex was established by the presence of characteristic M−$C_{carbene}$ ^{13}C NMR resonances at δ 162.4, 165.3, and 153.6 ppm for the Ni, Pd, and Pt complexes, respectively. The nickel complex was found to be diamagnetic, in line with a square-planar environment around the metal. Despite numerous attempts, no suitable X-ray-quality crystals could be grown for species $\mathbf{2_{Ni}}$, $\mathbf{2_{Pd}}$, and $\mathbf{2_{Pt}}$. Preliminary X-ray data collected for compound $\mathbf{2_{Pt}}$ were of insufficient quality for a refinement of the structure.[28] However, the atom connectivity could be unambiguously established.

Alternatively, the reaction of proligand **1** with $PtCl_2$ may be conducted in cyclohexylamine (as the solvent) to access the corresponding cyclohexylamine Pt complex $\mathbf{3_{Pt}}$. Thus, the reaction of benzimidazolium **1** with 1 equiv of $PtCl_2$ at 100 °C overnight quantitatively yielded the (NHC)Pt(cyclohexylamine) complex $\mathbf{3_{Pt}}$, as deduced from ^{1}H and ^{13}C NMR, mass spectrometry, and elemental analysis (Scheme 2). The synthesis of the Pt−DMSO adduct was next attempted following a similar strategy. The benzimidazolium salt cleanly reacted with $(DMSO)_2PtCl_2$ in acetonitrile and in the presence of NEt_3 acting as a base to afford the NHC platinum complex $\mathbf{4_{Pt}}$ as the major product (50% yield, Scheme 3), whose molecular structure was established through X-ray crystallography studies (Figure 1). Unexpectedly, the chelating ligand is

dx.doi.org/10.1021/om5003446 | *Organometallics* XXXX, XXX, XXX−XXX

Scheme 2. Synthesis of Platinum Complex 3_{Pt} in Cyclohexylamine as Solvent

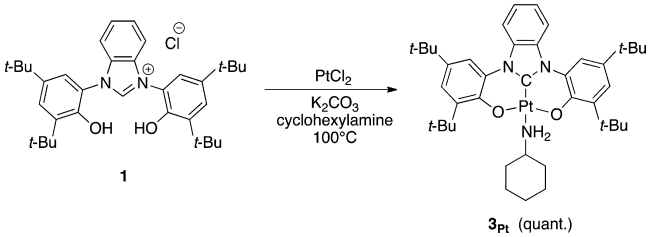

Scheme 3. Synthesis of Platinum Complex 4_{Pt} and Conversion into Complex 3_{Pt}

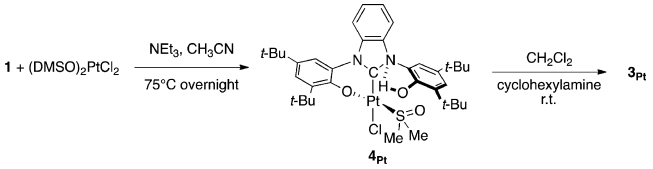

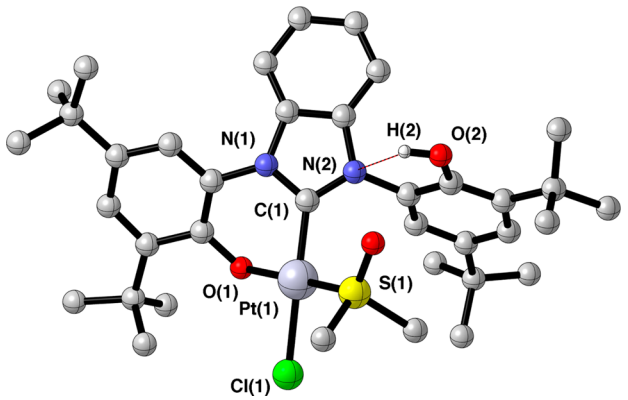

Figure 1. Molecular structure of the complex 4_{Pt}. Selected bond distances (Å) and angles (deg): C(1)−Pt(1), 1.950(9); O(1)−Pt(1), 2.016(6); Pt(1)−Cl(1), 2.350(3); S(1)−Pt(1), 2.201(2); N(2)···H(2), 2.310(9); N(2)−C(1)−N(1), 107.5(7); N(2)−C(1)−Pt(1), 127.9(6); N(1)−C(1)−Pt(1), 124.1(6); C(1)−Pt(1)−O(1), 85.0(3); C(1)−Pt(1)−S(1), 95.4(3); O(1)−Pt(1)−S(1), 174.14(17); C(1)−Pt(1)−Cl(1), 171.8(3); N(2)−C(1)−Pt(1)−O(1), −138.3(8); N(1)−C(1)−Pt(1)−O(1), 33.0(7); N(2)−C(1)−Pt(1)−S(1), 47.5(8).

κ^2(C,O)-coordinated with one "dangling" phenol forming an intramolecular hydrogen bond with a nitrogen atom of the N-heterocyclic ring (N···H = 2.310(9) Å). As a result, the dangling phenol points perpendicularly relative to the N-heterocyclic ring. The geometry around the Pt metal is square planar, with the chloride and DMSO ligands *trans* to the carbene and the phenolate, respectively. The carbene−Pt bond distance (1.950(9) Å) is similar to that in related complexes.[29] The M−$C_{carbene}$ ^{13}C NMR signal of 3_{Pt} was observed at 141.3 ppm.

Interestingly, a solution of 4_{Pt} in cyclohexylamine/dichloromethane as solvent led to the quantitative formation of the corresponding tridentate (OCO)Pt chelate complex 3_{Pt}, as deduced by NMR spectroscopy.

For comparison purposes, the coordination chemistry of the corresponding imidazolylidene type bis-aryloxide-NHC ligand **C** (Chart 1) was also studied. The azolium precursor **5** was easily prepared from the corresponding aminophenol (Scheme 4). Thus, the reaction of 2-amino-4,6-di-*tert*-butylphenol[5] with

Scheme 4. Synthesis of the Imidazolium Precursor 5

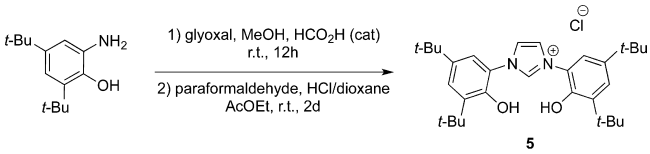

glyoxal in MeOH at room temperature followed by cyclization with paraformaldehyde and HCl afforded the desired product in 30% overall yield (not optimized).[30,31]

The imidazolium salt precursor **5** was then treated with 1 equiv of MCl_2 (M = Ni, Pd, Pt) in pyridine at 100 °C for 12 h to access the corresponding stable metal complexes **6** in 48−83% yield (Scheme 5). The formation of the corresponding

Scheme 5. Synthesis of Group 10 Complexes 6 and the Phosphine Complex 7_{Pt}

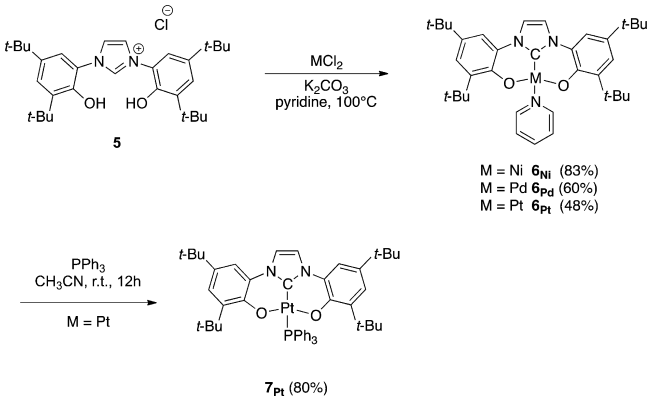

carbene complexes was confirmed by the presence of a carbene signal at δ 146.8, 149.8, and 153.5 ppm for the Ni, Pd, and Pt complexes, respectively, in the ^{13}C NMR spectra. X-ray-quality crystals of the nickel complex 6_{Ni} were grown as dark red prisms by diffusion of pentane into a dichloromethane solution of 6_{Ni} and allowed the determination of the molecular structure of species 6_{Ni} in the solid state. As shown in Figure 2, a square-planar environment at Ni is observed in complex 6_{Ni}, with an O−Ni−O bite angle of 177.44(11)°. The Ni−$C_{carbene}$ bond distance (1.794(3) Å) is comparable to those reported for other structurally related NHC−Ni complexes.[32] The {OCO}Ni chelate is significantly distorted from planarity (|(1)−N(1)−N(2)−O(2)| = 29.97(4)°). The Ni−$N_{pyridine}$ bond length (1.953(3) Å) is consistent with a *trans* influence of the carbene ligand.

Whereas pyridine exchange did not proceed with benzimidazolylidene complexes, we found that the corresponding imidazolylidene complexes were more susceptible to exchange reactions. For example, addition of 1 equiv of triphenylphosphine to the platinum compound 6_{Pt} afforded the corresponding phosphine adduct 7_{Pt} in 80% yield. X-ray-quality yellow prismatic crystals were grown by diffusion of pentane into a saturated solution of 7_{Pt} in dichloromethane, and X-ray diffraction studies allowed the structure determination of 7_{Pt}. As depicted in Figure 3, a distorted-square-planar environment around the metal is observed in species 7_{Pt}. The Pt−$C_{carbene}$ distance (1.948(3) Å) lies within the range of related structures.[29] Akin to the Ni complex, the {OCO}Pt chelate in the complex is significantly distorted from planarity (|O(1)−N(1)−N(2)−O(2)| = 28.60(4)°). The Pt−P bond length

dx.doi.org/10.1021/om5003446 | *Organometallics* XXXX, XXX, XXX−XXX

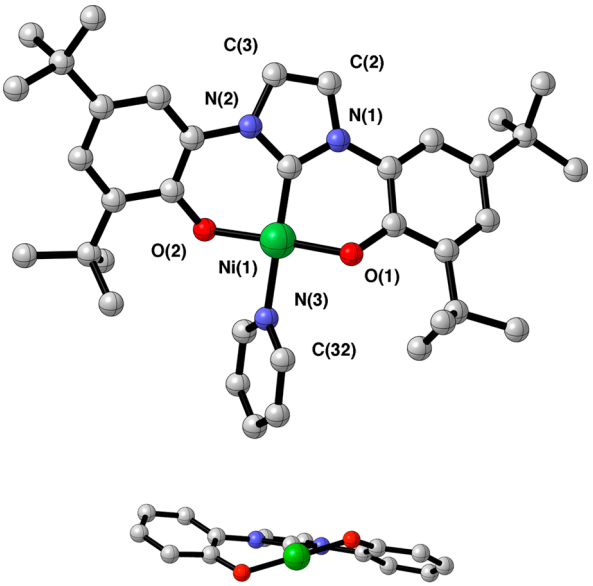

Figure 2. Molecular structure of the complex $\mathbf{6}_{Ni}$ (top) and view along the C−Ni axis (bottom; *t*-Bu groups and pyridine are omitted for clarity). Selected bond distances (Å) and angles (deg): C(1)−Ni(1), 1.794(3); N(3)−Ni(1), 1.953(3); O(1)−Ni(1), 1.847(2); O(2)−Ni(1), 1.835(2); N(1)−C(1)−N(2), 105.3(3); C(1)−Ni(1)−O(2), 91.48(14); C(1)−Ni(1)−O(1), 90.71(14); O(2)−Ni(1)−O(1), 177.44(11); C(1)−Ni(1)−N(3), 172.86(15); N(1)−C(1)−Ni(1)−O(2), −152.4(3); N(2)−C(1)−Ni(1)−O(2), 16.4(3); N(1)−C(1)−Ni(1)−O(1), 28.9(3); N(2)−C(1)−Ni(1)−O(1), −162.3(3); C(32)−N(3)−Ni(1)−O(1), 46.65(3); N(1)−C(2)−C(3)−N(2), −0.04(3).

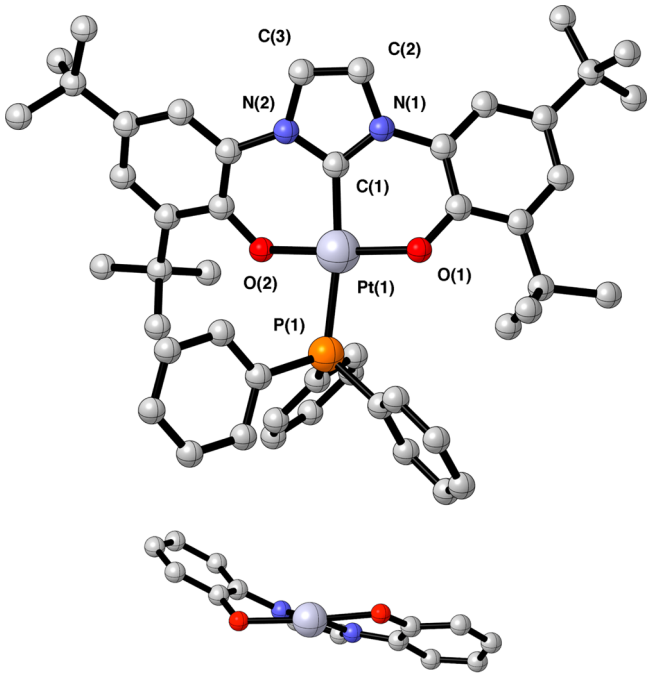

Figure 3. Molecular structure of the complex $\mathbf{7}_{Pt}$ (top) and view along the C−Pt axis (bottom; *t*-Bu groups and Ph_3P are omitted for clarity). Selected bond distances (Å) and angles (deg): C(1)−Pt(1), 1.948(3); O(1)−Pt(1), 2.006(2); O(2)−Pt(1), 2.017(2); P(1)−Pt(1), 2.3272(7); N(2)−C(1)−Pt(1), 126.3(2); N(1)−C(1)−Pt(1), 125.6(2); C(1)−Pt(1)−O(1), 89.27(10); C(1)−Pt(1)−O(2), 88.89(10); O(1)−Pt(1)−O(2), 175.73(8); C(1)−Pt(1)−P(1), 170.80(9); O(1)−Pt(1)−P(1), 85.96(6); O(2)−Pt(1)−P(1), 96.37(6); N(1)−C(1)−Pt(1)−O(1), 28.17(3); P(1)−O(1)−Pt(1)−C(1), 172.11(3).

(2.3272(7) Å) is consistent with a *trans* influence of the carbene ligand.

Ground-State Geometry and Frontier Orbitals. The minor extent of the SOC effect exerted by first-row transition metals and the presence of lower-lying energy MC states make Ni(II) complexes much less appealing for photophysical and theoretical studies; thus, such characterization has not been considered for complex $\mathbf{2}_{Ni}$. On the other hand, the molecular structures of the platinum(II) and palladium(II) derivatives $\mathbf{2}_{Pd-Pt}$ $\mathbf{3}_{Pt}$ $\mathbf{6}_{Pd-Pt}$ and $\mathbf{7}_{Pt}$ were optimized at their electronic ground state (S_0) by means of density functional theory (DFT) at the PBE0/(6-31G(d,p)+SDD) level, where the *tert*-butyl groups were replaced by methyl groups for shorter computational time. The Perdew−Burke−Erzenrhof parameter-free hybrid functional[33] (PBE0)[34] is well-known to properly describe the electronic and optical properties of phosphorescent platinum(II) complexes bearing chelating chromophoric ligands.[15f,18g,23a] The main computed geometrical parameters are given in Table S1 and the geometry is shown in Figure S1 (Supporting Information). The calculated S_0 structures are in good agreement with the geometrical parameters experimentally gathered from single-crystal X-ray diffractometric analyses.

For all complexes, the computed geometries display a distorted-square-planar coordination geometry around the metal atom, with either C_s (for complexes $\mathbf{2}_{Pd-Pt}$ $\mathbf{3}_{Pt}$ and $\mathbf{6}_{Pd-Pt}$) or C_1 (for complex $\mathbf{7}_{Pt}$) point group symmetry. The C_s-symmetric structures exhibit a σ mirror plane perpendicular to the O−C_{NHC}−O plane, bisecting the NHC moiety and containing the metal center. In particular, the DFT-optimized structures nicely reproduce the M−C^1 distances, (1.915−1.962 Å vs 1.948−1.950 Å for the computed and experimental distances, respectively; see Figure S1 in the Supporting Information for the corresponding atom labeling). Likewise, M−N^1 and M−O bond distances are in the ranges 2.134−2.151 and 1.992−2.018 Å (experimental 2.006 Å), respectively. The M−P^1 bond distance for $\mathbf{7}_{Pt}$ was found to be 2.369 Å (experimental 2.327 Å). Bond angle values are also in good agreement with crystallographic data and data for related cyclometalated platinum(II) and palladium(II) complexes previously reported. In particular, the C^1−M−O and N^1−M−O (P^1−M−O) angles are in the ranges 91.2−93.0 and 86.6−88.0° (86.1−91.4°), respectively. These values are very close to the ideal chelating arrangement for square-planar M(II) complexes (90°). Also, they are in good agreement with values for related tetradentate complexes bearing bis[phenolate(N-heterocyclic carbene)] recently reported by Che and co-workers[12c,19a] and Strassner and co-workers,[19b] confirming the suitability of the presently used computational model for describing the geometrical parameters of the complexes. In contrast with the reported tetradentate complexes,[12c,19] it is worth noting that in the case of $\mathbf{2}_{Pd-Pt}$ and $\mathbf{3}_{Pt}$ the benzimidazole ring is highly distorted in order to allow coordination of the bis-aryloxide moieties to the metal center. Two views of the optimized geometry for complex $\mathbf{2}_{Pt}$ are shown in Figure 4. Regarding derivatives $\mathbf{2}_{Pd-Pt}$ $\mathbf{3}_{Pt}$ and $\mathbf{6}_{Pd-Pt}$ at their S_0 optimized geometry, the ring of the ancillary pyridine ligand lies on the molecule plane as defined by the Pt−C^1, Pt−O^1, Pt−O^2, and Pt−N^1 coordination motifs (out-of-plane O−M−N^1−C^6 dihedral angles lying between 0.9 and 2.8°). Notably, this is in spite of the presence of bulky *tert*-butyl

dx.doi.org/10.1021/om5003446 | *Organometallics* XXXX, XXX, XXX−XXX

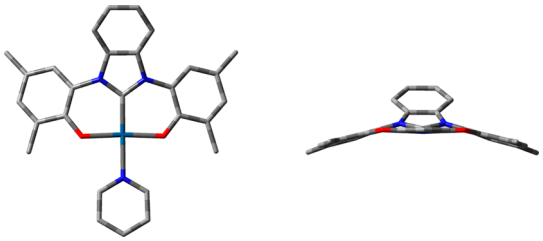

Figure 4. Two views of the S_0 optimized geometry of complex $\mathbf{2}_{Pt}$. Hydrogen atoms are omitted for clarity.

groups on the phenolate moieties at the ortho positions. Such a geometrical arrangement thus allows electronic communication between the d metal atom orbitals and the π electronic cloud of the pyridine ligand.

Figure 5 depicts the isodensity surface plots for the most relevant Kohn–Sham molecular orbitals (MOs) closer to the frontier region for the investigated complexes, and Figure S2 (Supporting Information) features a more complete list. In Table S2 (Supporting Information) are given the energies of the corresponding orbitals from HOMO-8 to LUMO+3, along with the HOMO–LUMO energy gap. The HOMO is an antibonding combination of the π orbitals of the two phenolate moieties and the d_{xz} orbitals of the metal atom with minor contribution of the N atom of the NHC moiety. The HOMO lies at −4.872, −4.768, −4.838, and −4.718 eV for $\mathbf{2}_{Pd}$, $\mathbf{2}_{Pt}$, $\mathbf{6}_{Pd}$, and $\mathbf{6}_{Pt}$, respectively. In particular, when pairs of complexes with the same ligands are considered, namely $\mathbf{2}_{Pd}/\mathbf{2}_{Pt}$ and $\mathbf{6}_{Pd}/\mathbf{6}_{Pt}$, palladium(II) derivatives show a HOMO stabilized by ca. 110 meV with respect to its platinum(II) counterparts. This finding can be ascribed to the higher oxidation potential of Pd(II) with respect to Pt(II).[35] As expected, the presence of a stronger donating ancillary ligand, such as triphenylphosphine, induces stabilization (of about 50–60 meV) with respect to the corresponding pyridine-containing complex: i.e., $\mathbf{6}_{Pt}$ vs $\mathbf{7}_{Pt}$. The more stable filled orbitals HOMO-1 and HOMO-2 involve other π orbitals of the two phenolate moieties and the C_{NHC} (for HOMO-1) and the π orbitals of the two phenolate and NHC moiety (for HOMO-2), with only minor contribution of the d metal orbitals.

On the other hand, the lowest unoccupied MOs LUMO and LUMO+1 show a π^* (pyridine) and π^* (phenyl(PPh_3)) character for pyridine- and triphenylphosphine-containing derivatives, respectively. This change in the nature of the LUMO is ascribed to the presence of low-lying π-antibonding orbitals of the pyridine with respect to the triphenylphosphine coordinating ligand, which in turn stabilizes the lowest-lying virtual orbital by 0.59 eV ($\mathbf{6}_{Pt}$ vs $\mathbf{7}_{Pt}$). Similarly, going from a cyclohexylamine ligand to pyridine in complex $\mathbf{3}_{Pt}$ yields a LUMO with d(Pt)π^*(benzimidazole) character. Overall, the LUMO lies at −1.274, −1.395, −0.810, −1.161, and −1.281 eV for $\mathbf{2}_{Pd}$, $\mathbf{2}_{Pt}$, $\mathbf{3}_{Pt}$, $\mathbf{6}_{Pd}$, and $\mathbf{6}_{Pt}$, respectively. When the same coordination sphere is retained and the metal ion is changed, it can be noted that platinum complexes show a smaller HOMO–LUMO gap energy: 3.598 vs 3.372 eV and 3.673 vs 3.438 eV for $\mathbf{2}_{Pd}$ vs $\mathbf{2}_{Pt}$ and $\mathbf{6}_{Pd}$ vs $\mathbf{6}_{Pt}$, respectively, which is due to the concomitant presence of the HOMO lying higher in energy and the more stabilized LUMO in Pt(II) vs Pd(II) complexes (see Table S2 in the Supporting Information).

Electronic Spectroscopy and TD-DFT. Figure 6 displays the electronic absorption spectra of complexes $\mathbf{2}_{Pt}$ and $\mathbf{6}_{Pt}$ in dichloromethane at a concentration of 5×10^{-5} M, and Figure S3 (Supporting Information) shows the corresponding absorption spectra for $\mathbf{2}_{Pd}$, $\mathbf{3}_{Pt}$, and $\mathbf{7}_{Pt}$. The photophysical data are given in Table 1. In order to shed light on the properties of the electronic transitions involved in the optical absorption processes, time-dependent density functional theory

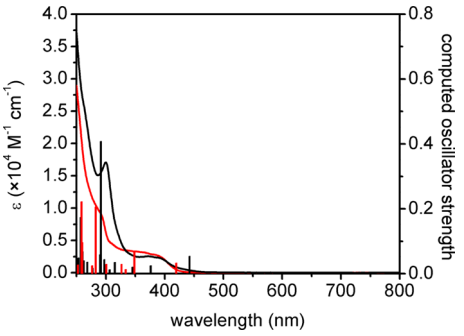

Figure 6. Comparison between the experimental absorption (solid line) spectrum in dichloromethane of complexes $\mathbf{2}_{Pt}$ (black trace) and $\mathbf{6}_{Pt}$ (red trace) and computed vertical transitions (vertical bars) with the corresponding oscillator strengths calculated in dichloromethane.

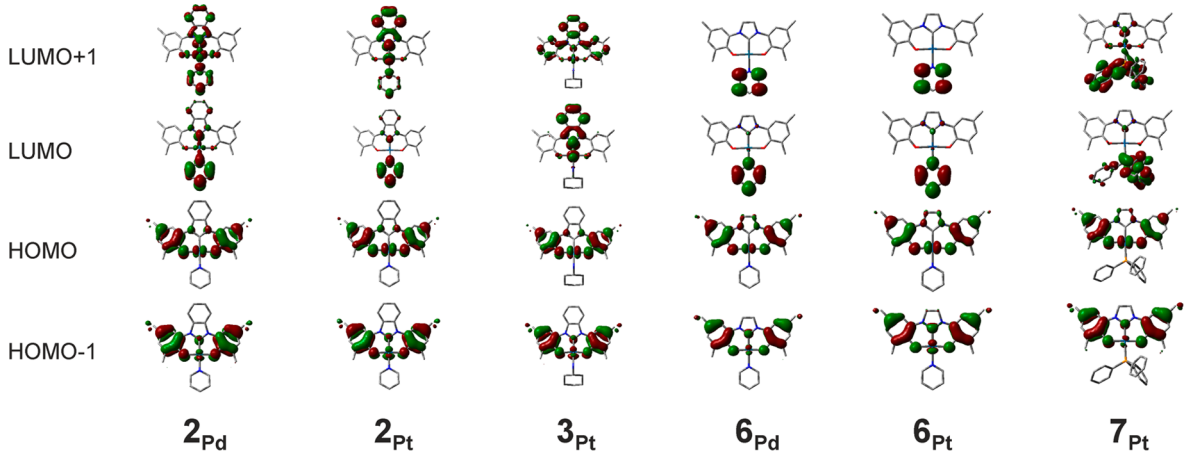

Figure 5. Isodensity surface plots of the molecular orbitals closer to the frontier region and mainly involved in the electronic transitions for the complexes $\mathbf{2}_{Pd}$, $\mathbf{6}_{Pd}$, $\mathbf{2}_{Pt}$, $\mathbf{3}_{Pt}$, $\mathbf{6}_{Pt}$, and $\mathbf{7}_{Pt}$ in the gas phase at their S_0 optimized geometries (isodensity value 0.035 e bohr^{-3}). Hydrogen atoms are omitted for clarity.

dx.doi.org/10.1021/om5003446 | Organometallics XXXX, XXX, XXX–XXX

Table 1. Electronic Absorption in Dilute CH_2Cl_2 Solution at Room Temperature and Photoluminescence in CH_2Cl_2/MeOH 1/3 Glassy Matrix at 77 K Characteristics for Complexes $\mathbf{2}_{Pt}$, $\mathbf{2}_{Pd}$, $\mathbf{3}_{Pt}$, $\mathbf{6}_{Pt}$, and $\mathbf{7}_{Pt}$

		77 K	
compound	room temp λ_{abs}, nm (ε, 10^4 M^{-1} cm^{-1})[a]	λ_{em}, nm	τ, μs
$\mathbf{2}_{Pt}$	260 sh (2.71), 300 (1.71), 372 (0.26), 390 (0.23)	507	1.1 (43%), 8.1 (57%)
$\mathbf{2}_{Pd}$	267 sh (2.39), 290 (2.12), 358 (0.43)	*b*	*b*
$\mathbf{3}_{Pt}$	263 sh (2.00), 298 (1.34), 374 (0.25), 413 (0.20)	519	1.4 (75%), 9.3 (25%)
$\mathbf{6}_{Pt}$	258 sh (2.10), 289 (0.95), 337 (0.34), 387 (0.27)	488	3.4 (26%), 12.8 (74%)
$\mathbf{7}_{Pt}$	275 sh (1.89), 365 (0.42), 383 (0.40)	*b*	*b*

[a]sh denotes a shoulder. [b]Not emissive.

(TD-DFT) was employed for the investigated complexes in both vacuum and dichloromethane as solvent by means of the IEFPCM solvation model. The computed vertical transitions were calculated at the S_0-optimized geometry and described in terms of one-electron excitations of molecular orbitals of the corresponding S_0 geometry. For the investigated complexes, the most relevant computed transitions involved in the vertical excitation processes along with their energy, character, and oscillator strengths are given in Tables S3 and S4 (Supporting Information) for singlet excitations and Tables S5 and S6 (Supporting Information) for triplet transitions, in both vacuum and CH_2Cl_2. For complexes $\mathbf{2}_{Pt}$ and $\mathbf{6}_{Pt}$ the computed transitions in CH_2Cl_2 are reported for comparison in Figure 6. Further computational details are available in the Experimental Section.

For complexes $\mathbf{2}_{Pt}$ and $\mathbf{6}_{Pt}$, the experimental electronic absorption spectra (CH_2Cl_2) contain a featureless and weak band ($\varepsilon \approx (2-3) \times 10^3$ M^{-1} cm^{-1}) between 350 and 450 nm that can be ascribed to the lowest-lying singlet-manifold metal-to-ligand charge transfer (^{1}MLCT) transition. On the basis of TD-DFT computations in CH_2Cl_2, it is possible to assign this weak band to the overlap of (i) an $S_0 \rightarrow S_1$ transition (HOMO → LUMO, f = 0.054 and 0.033 for $\mathbf{2}_{Pt}$ and $\mathbf{6}_{Pt}$, respectively) which essentially involves the π orbitals located on the phenoxy moiety, the platinum d orbital, and the π^* orbitals of pyridine (d(Pt) phenoxy → π^*(pyridine)) and (ii) transitions involving virtual orbitals mainly located on the NHC, i.e. d(Pt)π-(phenoxy) → π^*(NHC), and the combination of phenoxy and NHC, i.e. d(Pt)π(phenoxy) → π^*(phenoxy)π^*(NHC), for $\mathbf{2}_{Pt}$ and $\mathbf{6}_{Pt}$, respectively. The former can indeed be attributed to the HOMO → LUMO+1 (375 nm, f = 0.025) vertical transition and the latter to the HOMO → LUMO+2 (350 nm, f = 0.066) one-electron excitation process. The calculated lowest-energy values nicely correspond to the onset in the experimental absorption spectra that extends toward the lower energy side, confirming the suitability of the employed TD-DFT approach for the computation of such optically populated Franck–Condon excitations. At higher energies (λ <350), much more intense bands ($\varepsilon = (0.5-3) \times 10^4$ M^{-1} cm^{-1}) can be encountered at around 300 nm and are better described as an admixture of spin-allowed ligand-to-ligand charge transfer (^{1}LLCT) and ligand-centered (^{1}LC) transitions with small to negligible participation of the metal orbitals. In particular, very intense transitions are computed at 290 (f = 0.408) and 284 nm (f = 0.206) and mainly described as metal-perturbed ^{1}LC/^{1}LLCT d(Pt)π(phenoxy)π(NHC) → π^*-(phenoxy) π^*(pyridine) and ^{1}LLCT d(Pt)π(phenoxy)π(NHC) → π^*(pyridine) excitation processes for $\mathbf{2}_{Pt}$ and $\mathbf{6}_{Pt}$, respectively. As also shown in Figure 6, the computed transitions are in good agreement with the overall experimental absorption spectra. Furthermore, such assignments are in line with those in analogous platinum complexes bearing bis-[phenolate(N-heterocyclic carbene)] ligands.[19a]

Upon excitation in the ^{1}MLCT band at wavelengths in the range 350–450 nm, dilute samples (concentration of 5.0×10^{-5} M) in either CH_2Cl_2 or CH_3CN and spin-coated poly(methyl methacrylate) (PMMA) thin films at doping concentrations as high as 10 wt % of the investigated complexes did not show any detectable emission at room temperature. However, when the temperature was lowered to 77 K in a CH_2Cl_2/MeOH (1/3) glassy matrix and excitation carried out at 375 nm, complexes $\mathbf{2}_{Pt}$, $\mathbf{3}_{Pt}$, and $\mathbf{6}_{Pt}$ displayed a broad and featureless, yet weak, emission band in the bluish-green region of the visible spectrum. The corresponding photoluminescence spectra are displayed in Figure 7. In particular, complexes $\mathbf{2}_{Pt}$, $\mathbf{3}_{Pt}$, and $\mathbf{6}_{Pt}$ show emission maxima centered at 507, 519, and 488 nm, respectively. This finding together with the absence of photoluminescence upon only matrix rigidification (i.e., in PMMA thin films) also support the presence of a low-lying thermally populated quenching excited state close to the emitting state. Furthermore, the presence of bulky and prone-to-rotate *tert*-butyl groups on the phenate moieties might also be responsible for the fast and efficient radiationless deactivation of the photoexcited molecules at room temperature.[36] As expected for a lower temperature, emission decay measured under frozen conditions are long and fall in the time scale of a few microseconds, as typical of phosphorescent platinum(II) complexes showing charge transfer transitions with sizable metal participation, being τ_1 = 8.1 (57%) and τ_2 = 1.1 (43%), τ_1 = 1.4 (75%) and τ_2 = 9.3 (25%), and τ_1 = 12.8 (74%) and τ_2 = 3.4 (26%) μs for complexes $\mathbf{2}_{Pt}$, $\mathbf{3}_{Pt}$, and $\mathbf{6}_{Pt}$, respectively. On the basis of these findings, a ligand-centered (LC) transition responsible for this emission can be excluded.[37] Also, transition originating from a spin-forbidden distorted ligand field (LF) excited state can be ruled out, due to the fact that such a transition in platinum complexes generally shows a Gaussian-shaped broad emission profile with Stokes shift larger than those observed here.[38] Emission originating from excimer and aggregates can also be ruled out, due to the presence of bulky *tert*-butyl substituents. Thus, the radiative process

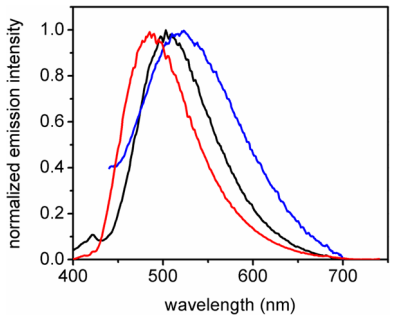

Figure 7. Emission spectra of complexes $\mathbf{2}_{Pt}$ (black trace), $\mathbf{3}_{Pt}$ (blue trace), and $\mathbf{6}_{Pt}$ (red trace) in CH_2Cl_2/MeOH 1/3 at 77 K glassy matrix at a concentration of 1.25×10^{-5} M. The samples were excited in the MLCT absorption band at λ_{exc} 375 nm.

dx.doi.org/10.1021/om5003446 | *Organometallics* XXXX, XXX, XXX–XXX

responsible for the emission can be ascribed to a triplet-manifold transition with sizable involvement of the d(Pt) orbitals and the π(phenoxy) as well as the π^* orbitals of either the pyridine or the NHC moiety for $\mathbf{2}_{Pt}/\mathbf{6}_{Pt}$ and $\mathbf{3}_{Pt}$, respectively. The nature of such a transition can be tentatively described as metal−ligand-to-ligand charge transfer (^{3}MLLCT).

In order to simulate the phosphorescence spectra and shed light on the electronic transition involved in such an emission process, the vertical (Franck−Condon) excitation energies for the optimized S_0 state to the lowest lying triplet manifold (T_1) were computed by means of TD-DFT at the same level of theory as for the ground state and the data for the $S_0 \rightarrow T_n$ (n = 1−3) are given in Tables S5 and S6 (Supporting Information). Such a method has been previously reported to successfully reproduce phosphorescence transitions in platinum complexes.[15f,18g,23a] The computed transitions ($S_0 \rightarrow T_1$) in dichloromethane as solvent medium lie at 2.59, 2.65, and 2.79 eV for $\mathbf{2}_{Pt}$, $\mathbf{3}_{Pt}$, and $\mathbf{6}_{Pt}$, respectively, and agree with the emission maxima recorded in 77 K glassy matrix, the experimental values being 2.45, 2.39, and 2.54 eV for $\mathbf{2}_{Pt}$, $\mathbf{3}_{Pt}$, and $\mathbf{6}_{Pt}$ respectively.[39] For all three complexes, such transitions can be mainly described as a one-electron excitation process involving a HOMO → LUMO transition: i.e., d(Pt)π(phenoxy) → π^*(pyridine) for $\mathbf{2}_{Pt}$ and $\mathbf{6}_{Pt}$ derivatives and d(Pt)π(phenoxy) → d*(Pt)π^*(NHC) for $\mathbf{3}_{Pt}$. These findings are in line with the assignment given on the basis of the experimental photophysical data as well as with closely related complexes.[12c] On going from complex $\mathbf{2}_{Pt}$ to $\mathbf{6}_{Pt}$, the 200 meV computed hypsochromic shift is mostly ascribed to the lower-lying LUMO in $\mathbf{6}_{Pt}$ vs $\mathbf{2}_{Pt}$. Such an assignment also rationalizes the absence of room-temperature luminescence of the investigated complexes. In all complexes, the (OCO)M chelate indeed adopts a highly distorted geometry around the metal center. In addition, in the case of derivatives $\mathbf{2}_{Pt}$, $\mathbf{2}_{Pd}$, and $\mathbf{3}_{Pt}$, the distortion is such that the benzimidazole moiety is not planar, giving rise to a significantly bent geometry (see above). Moreover, for species $\mathbf{2}_{Pt}$ and $\mathbf{6}_{Pt}$, the lowest-lying virtual orbital is located on a monodentate ancillary ligand relatively free to rotate. In all cases, upon photoexcitation the geometrical arrangement is such that the excited complexes are prone to easily deactivate via radiationless deactivation channels such as vibrational motion of the ancillary ligands as well as ligand decoordination.[40] However, when the temperature is lowered to 77 K, such nonradiative channels are partially suppressed, allowing radiative transitions to occur.

SUMMARY AND CONCLUSION

In summary, we have reported the direct and good-yielding synthesis and characterization of a series of group 10 complexes (Ni, Pd, Pt) bearing tridentate NHC ligands. Introduction of a benzimidazolylidene or imidazolylidene bis-aryloxide-NHC allowed their isolation and characterization in good yields. These compounds were investigated by means of DFT and TD-DFT computational methods, and the computed and experimental data match well. Frontier orbital analysis performed for all Pd and Pt complexes agrees with a HOMO centered on the metal and the aryloxide part of the ligand, while the LUMO is mainly located on the ancillary monodentate ligand, except for complex $\mathbf{3}_{Pt}$. No luminescence was observed for these complexes at room temperature (in CH_2Cl_2 or CH_3CN) upon excitation in the ^{1}MLCT band at wavelengths in the region 350−450 nm. The absence of luminescence is likely due to the distorted-square-planar structure of the (OCO)M chelate and the free rotation of the monodentate ancillary ligand. As a result, the excited complexes may readily undergo a radiationless deactivation after photoexcitation. Nevertheless, when the temperature was lowered to 77 K, pyridine- and cyclohexyl-containing platinum derivatives displayed an emission band in the green region of the visible spectrum attributable to a long-lived triplet-manifold excited state with MLLCT character.

EXPERIMENTAL SECTION

General Considerations. All reactions were performed under an inert atmosphere of argon or nitrogen using standard Schlenk line techniques. Solvents were purified and degassed by standard procedures. All other reagents were used without further purification. ^{1}H and ^{13}C nuclear magnetic resonance (NMR) spectra were recorded on a Bruker AVANCE 300 spectrometer using the residual solvent peak as reference ($CDCl_3$: δ(H) 7.26 ppm; δ(C) 77.16 ppm) at 298 K. MS ESI analyses were made on a microTOF instrument from Bruker Daltonics. Crystal data were collected at 173 K using Mo Kα graphite-monochromated (λ = 0.71073 Å) radiation on a Nonius KappaCCD diffractometer. The structures were solved using direct methods with SHELXS97. Non-hydrogen atoms were refined anisotropically. Hydrogen atoms were generated according to stereochemistry and refined using a riding model in SHELXL97 (except for H(2) in complex $\mathbf{4}_{Pt}$ which was located in the Fourier map).

Photophysical Characterization. Steady-state emission spectra at both room temperature in organic solvent and 77 K in 2-MeTHF glassy matrix were recorded on a HORIBA Jobin-Yvon IBH FL-322 Fluorolog 3 spectrometer equipped with a 450 W xenon arc lamp as the excitation source, double-grating excitation and emission monochromators (2.1 nm mm^{-1} of dispersion; 1200 grooves mm^{-1}), and a TBX-04 single-photon-counting device as the detector. Emission and excitation spectra were corrected for source intensity (lamp and grating) and emission spectral response (detector and grating) by standard correction curves. Time-resolved measurements were performed using the multichannel scaling electronics (MCS) option on the Fluorolog 3, where a pulsed xenon lamp used with a repetition rate of 30 Hz was used to excite the samples. The excitation sources were mounted directly on the sample chamber at 90° to a double-grating emission monochromator (2.1 nm mm^{-1} of dispersion; 1200 grooves mm^{-1}) and collected by a TBX-04 single-photon-counting detector. Signals were collected using an IBH Data Station Hub photon-counting module, and data analysis was performed using the commercially available DAS6 software (HORIBA Jobin Yvon IBH). The quality of the fit was assessed by minimizing the reduced χ^2 function and by visual inspection of the weighted residuals. For multiexponential decays, the intensity, namely $I(t)$, has been assumed to decay as the sum of individual single-exponential decays (eq 1):

$$I(t) = \sum_{i=1}^{n} \alpha_i \exp\left(-\frac{t}{\tau_i}\right) \quad (1)$$

where t_i values are the decay times and α_i values are the amplitudes of the components at t = 0. In the tables, the percentages for the pre-exponential factors, α_i, are given upon normalization. For multi-exponential decays, radiative and nonradiative rate constants were calculated with respect to the longer component. All solvents were spectrometric grade.

Computational Investigation. Ground-state (S_0) geometries were optimized by means of density functional theory (DFT), employing the Perdew−Burke−Erzenrhof parameter-free hybrid functional[33] PBE0, called PBE1PBE in Gaussian. The standard valence double-ζ polarized basis set 6-31G(d,p)[41] was used for C, H, N, and O for optimization. For Pt, the Stuttgart−Dresden (SDD) effective core potential was employed along with the corresponding valence triple-ζ basis set. The nature of all the stationary points was checked by computing vibrational frequencies, and all of the species were found to be true potential energy minima, as no imaginary frequencies were

dx.doi.org/10.1021/om5003446 | Organometallics XXXX, XXX, XXX−XXX

obtained. In order to simulate the absorption electronic spectrum down to about 250 nm, for all complexes the 30 lowest singlet ($S_0 \rightarrow S_n$, $n = 1-30$) as well as the 3 lowest triplet excitation energies ($S_0 \rightarrow T_n$, $n = 1-3$) were computed on the fully optimized geometry at the S_0 state by means of time-dependent density functional theory calculations (TD-DFT), at the same level of accuracy as for the ground state.[42] TD-DFT energy calculations were performed in both vacuum and dichloromethane as the solvent. Solvation effects were taken into account by means of the nonequilibrium IEFPCM model.[43] All calculations were performed with the Gaussian09W program package.[44]

Experimental Procedures and Product Characterization. *Benzimidazolium* ***1***. This compound was synthesized as reported in the literature.[26] ^{1}H NMR ($CDCl_3$, 300 MHz, 20 °C): δ 1.35 (s, 18H, $C(CH_3)_3$), 1.49 (s, 18H, $C(CH_3)_3$), 7.17 (d, J = 2.3 Hz, 2H, CH_{Ar}), 7.57 (d, J = 2.3 Hz, 2H, CH_{Ar}), 7.59−7.63 (m, 2H, CH_{Ar}), 7.65−7.69 (m, 2H, CH_{Ar}), 9.05 (s, 1H, CH_{imid}), 9.29 (bs, 2H, OH). ^{13}C NMR ($CDCl_3$, 75 MHz, 20 °C): δ 29.6 (6C, $C(CH_3)_3$), 31.4 (6C, $C(CH_3)_3$), 34.5 (2C, $C(CH_3)_3$), 35.8 (2C, $C(CH_3)_3$), 114.5 (2C, CH_{Ar}), 120.3 (2C, CH_{Ar}), 120.9 (2C, C_{Ar}), 126.8 (2C, CH_{Ar}), 127.7 (2C, CH_{Ar}), 132.3 (2C, C_{Ar}), 141.4 (1C, C_{imid}), 141.8 (2C, C_{Ar}), 143.0 (2C, C_{Ar}), 149.2 (2C, C_{Ar}). MS (positive ESI): $[M - Cl]^+$ calculated for $C_{35}H_{47}N_2O_2$ 527.36, found 527.36.

General Procedure for the Synthesis of the NHC Complexes ***2***, ***3***, *and* ***6***. A mixture of azolium salt (1 equiv), metal dichloride (1 equiv), and potassium carbonate (30 equiv) was suspended in pyridine or cyclohexylamine (1 mL/0.02 mmol of MCl_2). The mixture was sonicated for 10 min and stirred at 100 °C over 12 h under an argon atmosphere. The resulting suspension was concentrated under reduced pressure and then dissolved in dichloromethane; this solution was filtered through a Celite plug and concentrated under reduced pressure. The desired complex was purified by silica gel chromatography (dichloromethane/cyclohexane 1/1).

Synthesis of $\mathbf{2_{Ni}}$. Following the general procedure, 1,3-bis(3,5-di-*tert*-butyl-2-hydroxyphenyl)-1*H*-benzo[*d*]imidazol-3-ium chloride (61 mg, 0.11 mmol), $NiCl_2$ (14 mg, 0.11 mmol), and K_2CO_3 (450 mg, 3.3 mmol) afforded complex $\mathbf{2_{Ni}}$ (57 mg, 79%, green solid). ^{1}H NMR ($CDCl_3$, 300 MHz, 20 °C): δ 1.05 (s, 18H, $C(CH_3)_3$), 1.38 (s, 18H, $C(CH_3)_3$), 7.07 (d, J = 2.5 Hz, 2H, $CH_{phenoxy}$), 7.38−7.44 (m, 4H, CH_{Ar}), 7.76−7.80 (m, 3H, CH_{Ar}), 8.14−8.17 (m, 2H, $CH_{benzimidazole}$), 8.94 (d, J = 5.0 Hz, 2H, 2 NCH_{pyr}). ^{13}C NMR ($CDCl_3$, 75 MHz, 20 °C): δ 29.1 (6C, $C(CH_3)_3$), 31.7 (6C, $C(CH_3)_3$), 34.3 (2C, $C(CH_3)_3$), 35.1 (2C, $C(CH_3)_3$), 113.7 (2C, CH_{Ar}), 114.6 (2C, CH_{Ar}), 120.7 (2C, CH_{Ar}), 123.3 (2C, CH_{Ar}), 123.6 (2C, CH_{Ar}), 127.6, 132.8, 135.3, 137.7, 140.4, 150.3, 154.1, 162.4 (1C, $C_{carbene}$). MS (positive ESI): $[M + H]^+$ calculated for $C_{40}H_{50}N_3NiO_2$ 662.33, found 662.32. Anal. Calcd for $C_{40}H_{49}N_3NiO_2$: C, 72.51; H, 7.45; N, 6.34. Found: C, 72.69; H, 7.75; N, 5.94.

Synthesis of $\mathbf{2_{Pd}}$. Following the general procedure, 1,3-bis(3,5-di-*tert*-butyl-2-hydroxyphenyl)-1*H*-benzo[*d*]imidazol-3-ium chloride (50 mg, 0.089 mmol), $PdCl_2$ (16 mg, 0.089 mmol), and K_2CO_3 (368 mg, 2.66 mmol) afforded complex $\mathbf{2_{Pd}}$ (63 mg, 66%, yellow-brown solid). ^{1}H NMR ($CDCl_3$, 300 MHz, 20 °C): δ 1.31 (s, 18H, $C(CH_3)_3$), 1.39 (s, 18H, $C(CH_3)_3$), 7.20 (d, J = 2.4 Hz, 2H, CH_{ar}), 7.40−7.51 (m, 4H, CH_{ar}), 7.73 (d, J = 2.4 Hz, 2H, CH_{ar}), 7.88 (tt, J = 7.7 and 1.6 Hz, 1H, CH_{Pyr}), 8.15−8.19 (m, 2H, CH_{ar}), 8.89 (d, J = 4.8 Hz, 2H, CH_{Pyr}). ^{13}C NMR ($CDCl_3$, 75 MHz, 20 °C): δ 29.5 (6C, $C(CH_3)_3$), 31.8 (6C, $C(CH_3)_3$), 34.3 (2C, $C(CH_3)_3$), 35.6 (2C, $C(CH_3)_3$), 114.1 (2C, C_{Ar}), 116.2 (2C, C_{Ar}), 121.5 (2C, C_{Ar}), 123.7 (2C, C_{Ar}), 124.2 (2C, C_{Ar}), 128.5 (2C, C_{Ar}), 133.2 (2C, C_{Ar}), 135.7 (2C, C_{Ar}), 138.4 (2C, C_{Ar}), 140.5 (2C, C_{Ar}), 150.6 (2C, C_{Ar}), 157.1 (2C, C_{Ar}), 165.3 (1C, $C_{carbene}$). MS (positive ESI): $[M - e^-]^+$ calculated for $C_{40}H_{49}N_3O_2Pd$ 709.29, found 709.29. Anal. Calcd for $C_{40}H_{49}N_3O_2Pd$: C, 67.64; H, 6.95; N, 5.92. Found: C, 67.22; H, 6.66; N, 5.64.

Synthesis of $\mathbf{2_{Pt}}$. Following the general procedure, 1,3-bis(3,5-di-*tert*-butyl-2-hydroxyphenyl)-1*H*-benzo[*d*]imidazol-3-ium chloride (50 mg, 0.089 mmol), $PtCl_2$ (24 mg, 0.089 mmol), and K_2CO_3 (368 mg, 2.66 mmol) afforded complex $\mathbf{2_{Pt}}$ (53 mg, 75%, yellow solid). ^{1}H NMR ($CDCl_3$, 300 MHz, 20 °C): δ 1.35 (s, 18H, $C(CH_3)_3$), 1.36 (s, 18H, $C(CH_3)_3$), 7.15 (d, J = 1.2 Hz, 2H, $CH_{phenoxy}$), 7.41−7.44 (m, H, $CH_{benzimidazole}$), 7.54 (t, J = 7.6 Hz, 2H, CH_{Pyr}), 7.76 (d, J = 1.2 Hz, 2H, $CH_{phenoxy}$), 7.95 (tt, J = 7.7 and 1.6 Hz, 1H, CH_{Pyr}), 8.13−8.17 (m, 2H, CH_{ar}), 8.99 (d, J = 4.8 Hz, 2H, NCH_{Pyr}). ^{13}C NMR ($CDCl_3$, 75 MHz, 20 °C): δ 29.0 (6C, $C(CH_3)_3$), 31.7 (6C, $C(CH_3)_3$), 34.3 (2C, $C(CH_3)_3$), 35.6 (2C, $C(CH_3)_3$), 114.2 (2C, CH_{Ar}), 116.1 (2C, CH_{Ar}), 121.1 (2C, CH_{Ar}), 123.5 (2C, CH_{Ar}), 124.6 (2C, CH_{Pyr}), 128.0 (2C, C_{Ar}), 132.9 (2C, C_{Ar}), 136.6 (1C, CH_{Ar}), 138.6 (2C, CH_{Pyr}), 140.2 (2C, C_{Ar}), 151.0 (2C, CH_{Pyr}), 153.6 (1C, $C_{carbene}$), 157.4 (2C, C_{Ar}). MS (positive ESI): $[M - e^-]^+$ calculated for $C_{40}H_{49}N_3O_2Pt$ 798.35, found 798.35. Anal. Calcd for $C_{40}H_{49}N_3O_2Pt$: C, 60.13; H, 6.18; N, 5.26. Found: C, 60.01; H, 6.12; N, 4.98.

Synthesis of $\mathbf{3_{Pt}}$. Following the general procedure, 1,3-bis(3,5-di-*tert*-butyl-2-hydroxyphenyl)-1*H*-benzo[*d*]imidazol-3-ium chloride (106 mg, 0.19 mmol), $PtCl_2$ (30 mg, 0.19 mmol), and K_2CO_3 (779 mg, 5.64 mmol) afforded complex $\mathbf{3_{Pt}}$ (153 mg, quantitative, yellow solid). ^{1}H NMR ($CDCl_3$, 300 MHz, 20 °C): δ 1.11−1.37 (m, 26H, $C(CH_3)_3$ + $CH_{2\ CHA}$), 1.49 (s, 18H, $C(CH_3)_3$), 1.66−1.70 (m, 2H, $CH_{2\ CHA}$), 1.80−1.84 (m, 2H, $CH_{2\ CHA}$), 2.42−2.45 (m, 2H $CH_{2\ CHA}$), 3.20−3.22 (m, 2H $CH_{2\ CHA}$), 3.32−3.42 (m, 1H CH_{CHA}), 7.18 (d, J = 2 Hz, 2H, $CH_{phenoxy}$), 7.38−7.41 (m, 2H, $CH_{benzimidazole}$), 7.71 (d, J = 2 Hz, 2H, $CH_{phenoxy}$), 8.08−8.11 (m, 2H, $CH_{benzimidazole}$). ^{13}C NMR ($CDCl_3$, 75 MHz, 20 °C): δ 25.0 (2C, $CH_{2\ CHA}$), 25.3 (2C, $CH_{2\ CHA}$), 29.1 (6C, $C(CH_3)_3$), 31.8 (6C, $C(CH_3)_3$), 34.3 (2C, $C(CH_3)_3$), 35.6 (2C, $CH_{2\ CHA}$), 35.8 (2C, $C(CH_3)_3$), 53.8 (1C, CH_{CHA}), 114.2 (2C, CH_{Ar}), 116.2 (2C, CH_{Ar}), 121.0 (2C, CH_{Ar}), 123.4 (2C, CH_{Ar}), 127.4 (2C, C_{Ar}), 133.0 (2C, C_{Ar}), 136.3 (2C, C_{Ar}), 139.7 (2C, C_{Ar}), 152.7 (1C, $C_{carbene}$), 155.9 (2C, C_{Ar}). MS (positive-ESI): $[M - e^-]^+$ calculated for $C_{41}H_{57}N_3O_2Pt$ 818.41, found 818.41. Anal. Calcd for $C_{41}H_{57}N_3O_2Pt$: C, 60.13; H, 7.02; N, 5.13. Found: C, 59.78; H, 6.80; N, 4.94.

Synthesis of $\mathbf{4_{Pt}}$. 1,3-Bis(3,5-di-*tert*-butyl-2-hydroxyphenyl)-1*H*-benzo[*d*]imidazol-3-ium chloride (56 mg, 0.1 mmol), $PtCl_2(DMSO)_2$ (42 mg, 0.1 mmol), and NEt_3 (63 μL, 0.45 mmol) were stirred in CH_3CN under an inert atmosphere at 75 °C over 12 h. The volatiles were removed under vacuum, and the residue was purified on silica (DCM/cyclohexane 8/2). A 40 mg portion of $\mathbf{4_{Pt}}$ was obtained (50%, pale yellow solid). ^{1}H NMR ($CDCl_3$, 300 MHz, 20 °C): δ 1.43 (s, 9H, $C(CH_3)_3$), 1.45 (s, 9H $C(CH_3)_3$), 1.52 (s, 9H $C(CH_3)_3$), 1.58 (s, 9H, $C(CH_3)_3$), 2.28 (s, 3H, $CH_{3\ DMSO}$), 3.34 (s, 3H, $CH_{3\ DMSO}$), 7.16−7.19 (m, 1H, CH_{Ar}), 7.31−7.44 (m, 3H, CH_{Ar}), 7.59 (d, J = 2.3 Hz, 1H, CH_{Ar}), 7.64 (d, J = 2.3 Hz, 1H, CH_{Ar}), 7.59 (d, J = 2.5 Hz, 1H, CH_{Ar}), 7.92 (s, 1H, CH_{Ar}). ^{13}C NMR ($CDCl_3$, 75 MHz, 20 °C): δ 29.9 (3C, $C(CH_3)_3$), 30.2 (3C, $C(CH_3)_3$), 31.6 (3C, $C(CH_3)_3$), 31.8 (3C, $C(CH_3)_3$), 34.4 (1C, $C(CH_3)_3$), 34.9 (1C, $C(CH_3)_3$), 35.5 (1C, $C(CH_3)_3$), 35.7 (1C, $C(CH_3)_3$), 42.6 (1C, CH_3), 46.9 (1C, CH_3), 112.9 (1C, CH_{Ar}), 113.3 (1C, CH_{Ar}), 116.6 (1C, CH_{Ar}), 123.2 (1C, CH_{Ar}), 124.8 (1C, CH_{Ar}), 125.0 (1C, CH_{Ar}), 125.2 (1C, CH_{Ar}), 125.3 (1C, CH_{Ar}), 128.2 (1C, CH_{Ar}), 128.5 (1C, CH_{Ar}), 131.2 (1C, CH_{Ar}), 135.8 (1C, CH_{Ar}), 138.0 (1C, CH_{Ar}), 141.3 (1C, CH_{Ar}), 141.6 (1C, CH_{Ar}), 145.2 (1C, CH_{Ar}), 148.8 (1C, CH_{Ar}), 155.3 (1C, CH_{Ar}). MS (positive ESI): $[M + H]^+$ calculated for $C_{37}H_{52}ClN_2O_3PtS$ 834.30, found 834.30. Anal. Calcd for $C_{37}H_{51}ClN_2O_3PtS$: C, 53.26; H, 6.16; N, 3.36. Found: C, 52.82; H, 5.88; N, 3.09.

Synthesis of Imidazolium ***5***. 2-Amino-4,6-di-*tert*-butylphenol (1.580 g, 7.14 mmol), glyoxal (518 mg, 3.57 mmol), and formic acid (4 drops) were stirred at room temperature over 12 h. The corresponding diimine was filtered off, washed with cold MeOH, and used without any further purification and characterization. The resulting yellow solid was then dissolved in AcOEt, and paraformaldehyde (114 mg, 3.79 mmol) and 4 N HCl/dioxane (1.166 mL, 4.67 mmol) were introduced to the reaction mixture. After 2 days of stirring the volatiles were removed and the residue was purified on silica using DCM/MeOH (from 1/0 to 95/5). A 526 mg portion of **5** was obtained (30%, not optimized). ^{1}H NMR ($CDCl_3$, 300 MHz, 20 °C): δ 1.30 (s, 18H, $C(CH_3)_3$), 1.42 (s, 18H, $C(CH_3)_3$), 7.05 (d, J = 2.3, 2H, CH_{Ar}), 7.47 (d, J = 2.3, 2H, CH_{Ar}), 7.64 (s, 2H, CH), 8.40 (bs, 2H, OH), 8.83 (s, 1H, CH_{imid}). ^{13}C NMR ($CDCl_3$, 75 MHz, 20 °C): δ 29.6 (6C, $C(CH_3)_3$), 31.3 (6C, $C(CH_3)_3$), 34.4 (2C, $C(CH_3)_3$), 35.7 (2C, $C(CH_3)_3$), 119.5 (2C, CH), 123.8 (2C, C_{Ar}), 124.5 (2C, CH_{Ar}), 126.5 (2C, CH_{Ar}), 136.7 (1C, $CH_{carbene}$), 141.7 (2C,

dx.doi.org/10.1021/om5003446 | *Organometallics* XXXX, XXX, XXX−XXX

CH_{Ar}), 143.2 (2C, CH_{Ar}), 148.1 (2C, CH_{Ar}). MS (positive ESI): $[M - Cl]^+$ calculated for $C_{31}H_{45}N_2O_2$ 477.35, found 477.35.

Synthesis of $\mathbf{6_{Ni}}$. Following the general procedure, 1,3-bis(3,5-di-*tert*-butyl-2-hydroxyphenyl)-1*H*-imidazol-3-ium chloride (103 mg, 0.2 mmol), $NiCl_2$ (26 mg, 0.2 mmol), and K_2CO_3 (829 mg, 6 mmol) afforded complex $\mathbf{6_{Ni}}$ (102 mg, 83%, brown solid). ^{1}H NMR ($CDCl_3$, 300 MHz, 20 °C): δ 1.07 (s, 18H, $C(CH_3)_3$), 1.34 (s, 18H, $C(CH_3)_3$), 7.03 (d, J = 2.3 Hz, 2H, $CH_{Phenoxy}$), 7.19 (d, J = 2.3 Hz, 2H, $CH_{Phenoxy}$), 7.41 (t, J = 6.4 Hz, 2H, CH_{Pyr}), 7.69 (s, 2H, CH), 7.82 (t, J = 7.7 Hz, 1H, CH_{Pyr}), 9.07 (d, J = 4.7 Hz, 2H, NCH_{Pyr}). ^{13}C NMR ($CDCl_3$, 75 MHz, 20 °C): δ 29.0 (6C, $C(CH_3)_3$), 31.7 (6C, $C(CH_3)_3$), 34.1 (2C, $C(CH_3)_3$), 35.2 (2C, $C(CH_3)_3$), 111.3 (2C, CH), 115.9 (2C, CH_{Ar}), 120.9 (2C, CH_{Ar}), 123.4 (2C, CH_{Ar}), 125.0 (2C, CH_{Ar}), 135.5 (2C, CH_{Ar}), 137.5 (1C, CH_{Ar}), 140.2 (2C, CH_{Ar}), 146.8 (1C, $CH_{carbene}$), 150.4 (2C, CH_{Ar}), 151.5 (2C, CH_{Ar}). MS (positive ESI): $[M - e]^+$ calculated for $C_{36}H_{47}N_3NiO_2$ 611.3016, found 611.2863. Anal. Calcd for $C_{36}H_{47}N_3O_2Ni$: C, 70.60; H, 7.73; N, 6.86. Found: C, 70.27; H, 7.54; N, 6.65.

Synthesis of $\mathbf{6_{Pd}}$. Following the general procedure, 1,3-bis(3,5-di-*tert*-butyl-2-hydroxyphenyl)-1*H*-imidazol-3-ium chloride (145 mg, 0.28 mmol), $PdCl_2$ (50 mg, 0.28 mmol), and K_2CO_3 (1.169 g, 8.5 mmol) afforded $\mathbf{6_{Pd}}$ (142 mg, 76%, yellow solid). ^{1}H NMR ($CDCl_3$, 300 MHz, 20 °C): δ 1.38 (s, 18H, $C(CH_3)_3$), 1.39 (s, 18H, $C(CH_3)_3$), 7.20 (d, J = 2.3, 2H, $CH_{Phenoxy}$), 7.27 (d, J = 2.3, 2H, $CH_{Phenoxy}$), 7.46–7.51 (m, 2H, CH_{Pyr}), 7.75 (s, 2H, CH), 7.90 (tt, J = 7.5, 1.5 Hz, 1H, CH_{Pyr}), 9.08 (dd, J = 6.4, 1.5 Hz, 2H, NCH_{Pyr}). ^{13}C NMR ($CDCl_3$, 75 MHz, 20 °C): δ 29.5 (6C, $C(CH_3)_3$), 31.7 (6C, $C(CH_3)_3$), 34.2 (2C, $C(CH_3)_3$), 35.7 (2C, $C(CH_3)_3$), 113.1 (2C, CH), 116.9 (2C, CH_{Ar}), 121.8 (2C, CH_{Ar}), 124.0 (2C, CH_{Ar}), 126.3 (2C, CH_{Ar}), 135.9 (2C, CH_{Ar}), 138.2 (1C, CH_{Pyr}), 140.3 (2C, CH_{Ar}), 149.8 (1C, $CH_{carbene}$), 150.5 (2C, CH_{Ar}), 154.3 (2C, CH_{Ar}). MS (positive ESI): $[M - e]^+$ calculated for $C_{36}H_{47}N_3O_2Pd$ 659.2711, found 659.2711. Anal. Calcd for $C_{36}H_{47}N_3O_2Pd{\cdot}CH_2Cl_2$: C, 59.64; H, 6.63; N, 5.64. Found: C, 59.62; H, 6.50; N, 5.65.

Synthesis of $\mathbf{6_{Pt}}$. Following the general procedure, 1,3-bis(3,5-di-*tert*-butyl-2-hydroxyphenyl)-1*H*-imidazol-3-ium chloride (193 mg, 0.38 mmol), $PtCl_2$ (100 mg, 0.38 mmol), and K_2CO_3 (1.559 g, 11.3 mmol) afforded $\mathbf{6_{Pt}}$ (134 mg, 48%, yellow solid). ^{1}H NMR ($CDCl_3$, 300 MHz, 20 °C): δ 1.33 (s, 18H, $C(CH_3)_3$), 1.34 (s, 18H, $C(CH_3)_3$), 7.13 (d, J = 2.4, 2H, $CH_{Phenoxy}$), 7.23 (d, J = 2.4, 2H, $CH_{Phenoxy}$), 7.52 (td, J = 6.5, 1.1 Hz, 2H, CH_{Pyr}), 7.67 (s, 2H, CH), 7.95 (tt, J = 7.7, 1.1 Hz, 1H, CH_{Pyr}), 9.08 (d, J = 6.5 Hz, 2H, NCH_{Pyr}). ^{13}C NMR ($CDCl_3$, 75 MHz, 20 °C): δ 29.5 (6C, $C(CH_3)_3$), 31.6 (6C, $C(CH_3)_3$), 34.1 (2C, $C(CH_3)_3$), 35.8 (2C, $C(CH_3)_3$), 113.0 (2C, CH), 115.7 (2C, CH_{Ar}), 121.3 (2C, CH_{Ar}), 124.4 (2C, CH_{Ar}), 126.0 (2C, CH_{Ar}), 136.7 (2C, CH_{Ar}), 138.3 (1C, CH_{Pyr}), 140.2 (2C, CH_{Ar}), 150.9 (2C, CH_{Ar}), 153.5 (1C, $CH_{carbene}$). MS (positive ESI): $[M]^+$ calculated for $C_{36}H_{47}N_3O_2Pt$ 748.33, found 748.33. Anal. Calcd for $C_{36}H_{47}N_3O_2Pt{\cdot}0.33CH_2Cl_2$: C, 56.15; H, 6.18; N, 5.41. Found: C, 55.97; H, 6.04; N, 5.37.

Synthesis of $\mathbf{7_{Pt}}$. Complex $\mathbf{6_{Pt}}$ (80 mg, 0.11 mmol) and triphenylphosphine (140 mg, 0.53 mmol) were stirred in CH_3CN over 12 h. The volatiles were removed under vacuum, and the residue was purified by column chromatography (DCM/cyclohexane 5/5 to 8/2). A 79 mg portion of $\mathbf{7_{Pt}}$ was obtained (80%, pale yellow solid). ^{1}H NMR ($CDCl_3$, 300 MHz, 20 °C): δ 0.73 (s, 18H, $C(CH_3)_3$), 1.33 (s, 18H, $C(CH_3)_3$), 7.01 (d, J = 2.4 Hz, 2H, $CH_{Phenoxy}$), 7.21 (d, J = 2.4 Hz, 2H, $CH_{Phenoxy}$), 7.33–7.44 (m, 9H, CH_{PPh3}), 7.73 (d, J = 1.1 Hz, 2H, CH), 7.84–7.90 (m, 6H, CH_{PPh_3}). ^{13}C NMR ($CDCl_3$, 75 MHz, 20 °C): δ 29.4 (6C, $C(CH_3)_3$), 31.6 (6C, $C(CH_3)_3$), 34.1 (2C, $C(CH_3)_3$), 35.1 (2C, $C(CH_3)_3$), 113.1 (2C, CH_{Ar}), 116.2 (2C, J_{C-P} = 4.9 Hz, C_{Ar}), 121.5 (2C, CH_{Ar}), 125.9 (2C, C_{Ar}), 128.3 (J_{C-P} = 10.3 Hz, C_{Ar}), 130.2 (J_{C-P} = 2.2 Hz, CH_{Ar}), 132.5 (J_{C-P} = 46.4 Hz, CH_{Ar}), 135.6 (J_{C-P} = 12.0 Hz, CH_{Ar}), 136.6 (2C, C_{Ar}), 141.0 (2C, CH_{Ar}), 149.9 (1C, J_{C-P} = 141 Hz, $C_{Carbene}$), 153.2 (2C, J_{C-P} = 1.6 Hz, C_{Ar}). ^{31}P NMR ($CDCl_3$, 120 MHz, 20 °C): δ 23.86 (J_{P-Pt} = 1411 Hz). MS (positive ESI): $[M + H]^+$: calculated for $C_{49}H_{58}N_2O_2Pt$ 932.39, found 932.38. Anal. Calcd for $C_{49}H_{57}N_2O_2PPt{\cdot}CH_2Cl_2$: C, 59.05; H, 5.85; N, 2.75. Found: C, 59.68; H, 5.92; N, 2.90.

■ ASSOCIATED CONTENT

Ⓢ Supporting Information

Figures, tables, and CIF and xyz files giving electronic absorption spectra for complexes $\mathbf{2_{Pd}}$, $\mathbf{3_{Pt}}$, and $\mathbf{7_{Pt}}$, additional computational data, all computed molecule Cartesian coordinates in a format for convenient visualization, NMR spectra for all compounds prepared in this paper, and crystallographic data for $\mathbf{4_{Pt}}$, $\mathbf{6_{Ni}}$, and $\mathbf{7_{Pt}}$. This material is available free of charge via the Internet at http://pubs.acs.org.

■ AUTHOR INFORMATION

Corresponding Authors

*E-mail for M.M.: mauro@unistra.fr.
*E-mail for S.D.: dagorne@unistra.fr.
*E-mail for S.B.-L.: bellemin@unistra.fr.

Notes

The authors declare no competing financial interest.

■ ACKNOWLEDGMENTS

The authors gratefully acknowledge the CNRS and the Ministère de l'Enseignement Supérieur et de la Recherche (MESR) for a PhD grant to G.D. The authors also thank Dr. C. Bailly and Dr. L. Brelot for X-ray diffraction studies (Strasbourg). M.M. gratefully acknowledges Prof. L. De Cola for allowing the use of the spectroscopy laboratory facilities and computational machine time.

■ REFERENCES

(1) (a) Nolan, S. P. *N-Heterocyclic Carbenes in Synthesis*; Wiley-VCH: Weinheim, Germany, 2006. (b) Glorius, F. *N-Heterocyclic Carbenes in Transition Metal Catalysis*; Springer-Verlag: Berlin, 2007. (c) Díez-González, S. *N-Heterocyclic Carbenes, From Laboratories Curiosities to Efficient Synthetic Tools*; RSC Publishing: Cambridge, U.K., 2011; RSC Catalysis Series.

(2) Selected reviews: (a) Bourissou, D.; Guerret, O.; Gabbaï, F.; Bertrand, G. *Chem. Rev.* **2000**, *100*, 39. (b) Herrmann, W. A. *Angew. Chem.* **2002**, *114*, 1342; *Angew. Chem., Int. Ed.* **2002**, *41*, 1290. (c) Hahn, F. E.; Jahnke, M. C. *Angew. Chem., Int. Ed.* **2008**, *47*, 3122. (d) Melaimi, M.; Soleilhavoup, M.; Bertrand, G. *Angew. Chem., Int. Ed.* **2010**, *49*, 8810.

(3) Selected reviews: (a) Perry, M. C.; Burgess, K. *Tetrahedron: Asymmetry* **2003**, *14*, 951. (b) César, V.; Bellemin-Laponnaz, S.; Gade, L. H. *Chem. Soc. Rev.* **2004**, *33*, 619. (c) Gade, L. H.; Bellemin-Laponnaz, S. *Top. Organomet. Chem.* **2007**, *21*, 117. (d) Wang, F.; Liu, L.-J.; Wang, W.; Li, S.; Shi, M. *Coord. Chem. Rev.* **2012**, *256*, 804. (e) Poyatos, M.; Mata, J. A.; Peris, E. *Chem. Rev.* **2009**, *109*, 3677. (f) de Frémont, P.; Marion, N.; Nolan, S. P. *Coord. Chem. Rev.* **2009**, *253*, 862. (g) Crabtree, R. H. *Coord. Chem. Rev.* **2013**, *257*, 755. (h) Donnelly, K. F.; Petronilho, A.; Albrecht, M. *Chem. Commun.* **2013**, *49*, 1145. (i) Fliedel, C.; Schnee, G.; Avilés, T.; Dagorne, S. *Coord. Chem. Rev.* **2014**, *275*, 63.

(4) Mercs, L.; Albrecht, M. *Chem. Soc. Rev.* **2010**, *39*, 1903.

(5) (a) Sun, R. W.-Y.; Chow, A. L.-F.; Li, X.-H.; Yan, J. J.; Chui, S. S.-Y.; Che, C.-M. *Chem. Sci.* **2011**, *2*, 728. (b) Liu, W.; Gust, R. *Chem. Soc. Rev.* **2013**, *42*, 755.

(6) (a) Zou, T.; Lok, C.-N.; Fung, Y. M. E.; Che, C.-M. *Chem. Commun.* **2013**, *49*, 5423. (b) Mauro, M.; Aliprandi, A.; Septiadi, D.; Kehr, S.; De Cola, L. *Chem. Soc. Rev.* **2014**, *43*, 4144 and references therein.

(7) (a) Wang, X.; Sobota, M.; Kohler, F. T. U.; Morain, B.; Melcher, B. U.; Laurin, M.; Wasserscheid, P.; Libuda, J.; Meyer, K. *J. Mater. Chem.* **2012**, *22*, 1893. (b) Huang, R. T. W.; Wang, W. C.; Yang, R. Y.; Lu, J. T.; Lin, I. J. B *Dalton Trans.* **2009**, 7121.

(8) (a) Tam, A. Y.-Y.; Yam, V. W.-W. *Chem. Soc. Rev.* **2013**, *42*, 1540. (b) Peterlik, H.; Weisbarth, R.; Nieger, M.; Dötz, K. H. *Angew. Chem.,*

Int. Ed. **2007**, *46*, 6368. (c) Hsu, T. H. T.; Naidu, J. J.; Yang, B.-J.; Jang, M.-Y.; Lin, I. J. B. *Inorg. Chem.* **2012**, *51*, 98.
(9) Visbal, R.; Gimeno, M. C. *Chem. Soc. Rev.* **2014**, *43*, 3551.
(10) Díez-González, S.; Marion, N.; Nolan, S. P. *Chem. Rev.* **2009**, *109*, 3612.
(11) (a) Sun, R. W.-Y.; Chow, A. L.-F.; Li, X.-H.; Yan, J. J.; Chui, S. S.-Y.; Che, C.-M. *Chem. Sci.* **2011**, *2*, 728−736. (b) Li, K.; Guan, X.; Ma, C.-W.; Lu, W.; Chen, Y.; Che, C.-M. *Chem. Commun.* **2011**, *47*, 9075.
(12) (a) Sajoto, T.; Djurovich, P. I.; Tamayo, A.; Youssufuddin, M.; Bau, R.; Thompson, M. E. *Inorg. Chem.* **2005**, *44*, 7992. (b) Chang, C.-F.; Cheng, Y.-M.; Chi, Y.; Chiu, Y.-C.; Lin, C.-C.; Lee, G.-H.; Chou, P.-T.; Chen, C.-C.; Chang, C.-H.; Wu, C.-C. *Angew. Chem., Int. Ed.* **2008**, *47*, 4542. (c) Li, K.; Cheng, G.; Ma, C.; Guan, X.; Kwok, W.-M.; Chen, Y.; Lu, W.; Che, C.-M. *Chem. Sci.* **2013**, *4*, 2630. (d) Darmawan, N.; Yang, C.-H.; Mauro, M.; Raynal, M.; Heun, S.; Pan, J.; Buchholz, H.; Braunstein, P.; De Cola, L. *Inorg. Chem.* **2013**, *52*, 10756. (e) Yang, C.-H.; Beltran, J.; Lemaur, V.; Cornil, J.; Harmann, D.; Sarfert, W.; Fröhlich, R.; Bizzarri, C.; De Cola, L. *Inorg. Chem.* **2010**, *49*, 9891. (f) Unger, Y.; Zeller, A.; Ahrens, S.; Strassner, T. *Chem. Commun.* **2008**, 3263. (g) Tronnier, A.; Strassner, T. *Dalton Trans.* **2013**, *42*, 9847. (h) Zhang, X.; Wright, A. M.; DeYonker, N. J.; Hollis, T. K.; Hammer, N. I.; Webster, C. E.; Valente, E. J. *Organometallics* **2012**, *31*, 1664. (i) Monti, F.; Kassler, F.; Delgado, M.; Frey, J.; Bazzanini, F.; Accorsi, G.; Armaroli, N.; Bolink, H. J.; Orti, E.; Scopelliti, R.; Nazeeruddin, M. K.; Baranoff, E. *Inorg. Chem.* **2013**, *52* (18), 10292.
(13) Baldo, M. A.; O'Brien, D. F.; You, Y.; Shoustikov, A.; Silbley, S.; Thompson, M. E.; Forrest, S. R. *Nature* **1998**, *395*, 151.
(14) (a) Sajoto, T.; Djurovich, P.; Tamayo, A. B.; Oxgaard, J.; Goddard, W. A., III; Thompson, M. E. *J. Am. Chem. Soc.* **2009**, *131*, 9813. (b) Kawamura, Y.; Goushi, K.; Brooks, J.; Brown, J. J.; Sasabe, H.; Adachi, C. *Appl. Phys. Lett.* **2005**, *86*, 071104. (c) Lin, C.-H.; Chang, Y.-Y.; Hung, J.-Y.; Lin, C.-Y.; Chi, Y.; Chung, M. W.; Lin, C. L.; Chu, P.-T.; Lee, G.-H.; Chang, C.-H.; Lin, W.-C. *Angew. Chem., Int. Ed.* **2011**, *50*, 3182. (d) Hang, X.-C.; Fleetham, T.; Turner, E.; Brooks, J.; Li, J. *Angew. Chem., Int. Ed.* **2013**, *52*, 6753. (e) Turner, E.; Bakken, N.; Li, J. *Inorg. Chem.* **2013**, *52*, 7344. (f) Kui, S. C. F.; Chow, P. K.; Cheng, G.; Kwok, C.-C.; Kwong, C. L.; Low, K.-H.; Che, C.-M. *Chem. Commun.* **2013**, *49*, 1497. (g) Hudson, Z. M.; Sun, C.; Helander, M. G.; Amarne, H.; Lu, Z.-H.; Wang, S. *Adv. Funct. Mater.* **2010**, *20*, 3426.
(15) (a) *Highly Efficient OLEDs with Phosphorescent Materials*; Yersin, H., Ed.; Wiley-VCH: Weinheim, Germany, 2008. (b) Thompson, M. E.; Djurovich, P. E.; Barlow, S.; Marder, S. Organometallic Complexes for Optoelectronic Applications. In *Comprehensive Organometallic Chemistry III*; Crabtree, R. H., Mingos, D. M. P., Eds.; Elsevier: Oxford, U.K., 2006. (c) Costa, R. D.; Ortí, E.; Bolink, H. J.; Monti, F.; Accorsi, G.; Armaroli, N. *Angew. Chem., Int. Ed.* **2012**, *51*, 8178. (d) Hu, T.; He, L.; Duan, L.; Qiu, Y. *J. Mater. Chem.* **2012**, *22*, 4206. (e) Xiao, L.; Chen, Z.; Qu, B.; Luo, J.; Kong, S.; Gong, Q.; Kido, J. *Adv. Mater.* **2011**, *23*, 926. (f) Cebrián, C.; Mauro, M.; Kourkoulos, D.; Mercandelli, P.; Hertel, D.; Meerholz, K.; Strassert, C. A.; De Cola, L. *Adv. Mater.* **2013**, *25*, 437. (g) Mydlak, M.; Bizzarri, C.; Hartmann, D.; Sarfert, W.; Schmid, G.; De Cola, L. *Adv. Funct. Mater.* **2010**, *20*, 1812. (h) Wang, R.; Liu, D.; Ren, H.; Zhang, T.; Wang, X.; Li, J. *J. Mater. Chem.* **2011**, *21*, 15494. (i) Tam, A. Y.-Y.; Tsang, D. P.-K.; Chan, M.-Y.; Zhu, N.; Yam, V. W.-W. *Chem. Commun.* **2011**, *47*, 3383. (j) Fleetham, T.; Ecton, J.; Wang, Z.; Bakken, N.; Li, J. *Adv. Mater.* **2013**, *25*, 2573.
(16) (a) Yang, C.-H.; Mauro, M.; Polo, F.; Watanabe, S.; Munster, I.; Frohlich, R.; De Cola, L. *Chem. Mater.* **2012**, *24*, 3684. (b) Ladouceru, S.; Swanick, K. N.; Gallagher-Duval, S.; Ding, Z.; Zysman-Colman, E. *Eur. J. Inorg. Chem.* **2013**, *30*, 5329. (c) Fernandez-Hernandez, J. M.; Ladouceur, S.; Shen, Y.; Iordache, A.; Wang, X.; Donato, L.; Gallagher-Duval, S.; de Anda Villa, M.; Slinker, J. D.; De Cola, L.; Zysman-Colman, E. *J. Mater. Chem. C* **2013**, *1*, 7440. (d) Lee, S. J.; Park, K. M.; Yang, K.; Kang, Y. *Inorg. Chem.* **2009**, *48*, 1030. (e) Chang, C.-H.; Wu, Z.-J.; Chiu, C.-H.; Liang, Y.-H.; Tsai, Y.-S.; Liao, J.-L.; Chi, Y.; Hsieh, H.-Y.; Kuo, T.-Y.; Lee, G.-H.; Pan, H.-A.; Chou, P.-T.; Lin, J.-S.; Tseng, M.-R. *ACS Appl. Mater. Interfaces* **2013**, *5*, 7341. (f) Chiu, Y.-C.; Hung, J.-Y.; Chi, Y.; Chen, C.-C.; Chang, C.-H.; Wu, C.-C; Cheng, Y.-M.; Yu, Y.-C.; Lee, G.-H.; Chou, P.-T. *Adv. Mater.* **2009**, *21*, 2221. (g) Yang, C.-H.; Cheng, Y.-M.; Chi, Y.; Hsu, C.-J.; Fang, F.-C.; Wong, K.-T.; Chou, P.-T.; Chang, C.-H.; Tsai, M.-H; Wu, C.-C. *Angew. Chem., Int. Ed.* **2007**, *46*, 2418.
(17) (a) Caspar, J. V.; Kober, E. M.; Sullivan, B. P.; Meyer, T. J. *J. Am. Chem. Soc.* **1982**, *104*, 630 and references therein. (b) Caspar, J. V.; Meyer, T. J. *J. Phys. Chem.* **1983**, *87*, 952. (c) Siebrand, W. J. *J. Chem. Phys.* **1966**, *48*, 2732. (d) Avouris, P.; Gelbart, W. M.; El-Sayed, M. A. *Chem. Rev.* **1977**, *77*, 793.
(18) (a) McGuire, R.; McGuire, M. C.; McMillin, D. R. *Coord. Chem. Rev.* **2010**, *254*, 2574. (b) Williams, J. A. G. *Coord. Chem. Rev.* **2008**, *252*, 2596. (c) Lai, S.-W.; Che, C.-M. *Top. Curr. Chem.* **2004**, *241*, 27. (d) Tong, G. S.-M.; Che, C.-M. *Chem. Eur. J.* **2009**, *15*, 7225. (e) Wong, K. M.-C.; Yam, V. W.-W. *Coord. Chem. Rev.* **2007**, *251*, 2477. (f) Rausch, A. F.; Murphy, L.; Williams, J. A. G.; Yersin, H. *Inorg. Chem.* **2012**, *51*, 312. (g) Wang, K.-W.; Chen, J.-L.; Cheng, Y.-M.; Chung, M.-W.; Hsieh, C.-C.; Lee, G.-H.; Chou, P.-T.; Chen, K.; Chi, Y. *Inorg. Chem.* **2010**, *49*, 1372.
(19) (a) Li, K.; Guan, X.; Ma, C.-W.; Lu, W.; Chen, Y.; Che, C.-M. *Chem. Commun.* **2011**, *47*, 9075. (b) Meyer, A.; Unger, Y.; Poethig, A.; Strassner, T. *Organometallics* **2011**, *30*, 2980.
(20) (a) Mróz, W.; Botta, C.; Giovanella, U.; Rossi, E.; Colombo, A.; Dragonetti, C.; Roberto, D.; Ugo, R.; Valore, A.; Williams, J. A. G. *J. Mater. Chem.* **2011**, *21*, 8653. (b) Ma, B.; Djurovich, P. I.; Garon, S.; Alleyne, B.; Thompson, M. E. *Adv. Mater.* **2006**, *16*, 2438.
(21) (a) Wong, K. M. C.; Yam, V. W. W. *Acc. Chem. Res.* **2011**, *44*, 424. (b) Leung, S. Y. L.; Lam, W. H.; Yam, V. W.-W. *Proc. Natl. Acad. Sci. U.S.A.* **2013**, *11*, 7986. (c) Miskowski, V. M.; Houlding, V. H. *Coord. Chem. Rev.* **1991**, *111*, 145. (d) Roundhill, D. M.; Gray, H. B.; Che, C.-M. *Acc. Chem. Res.* **1989**, *22*, 55. (e) Pyykkö, P. *Chem. Rev.* **1997**, *97*, 597.
(22) (a) Mauro, M.; Aliprandi, A.; Cebrián, C.; Wang, D.; Kübel, C.; De Cola, L. *Chem. Commun.* **2014**, *50*, 7269−7272. (b) Strassert, C. A.; Chien, C.-H.; Galvez Lopez, M. D.; Kourkoulos, D.; Hertel, D.; Meerholz, K.; De Cola, L. *Angew. Chem., Int. Ed.* **2011**, *50*, 946. (c) Komiya, N.; Okada, M.; Fukumoto, K.; Jomori, D.; Naota, T. *J. Am. Chem. Soc.* **2011**, *133*, 6493.
(23) (a) Mydlak, M.; Mauro, M.; Polo, F.; Felicetti, M.; Leonhardt, J.; Diener, G.; De Cola, L.; Strassert, C. A. *Chem. Mater.* **2011**, *23*, 3659. (b) Rothe, C.; Chiang, C.-J.; Jankus, V.; Abdullah, K.; Zeng, X.; Jitchati, R.; Batsanov, A. S.; Bryce, M. R.; Monkman, A. P. *Adv. Funct. Mater.* **2009**, *19*, 2038.
(24) (a) Bellemin-Laponnaz, S.; Welter, R.; Brelot, L.; Dagorne, S. *J. Organomet. Chem.* **2009**, *694*, 604. (b) Romain, C.; Brelot, L.; Bellemin-Laponnaz, S.; Dagorne, S. *Organometallics* **2010**, *29*, 1191. (c) Romain, C.; Miqueu, K.; Sotiropoulos, J.-M.; Bellemin-Laponnaz, S.; Dagorne, S. *Angew. Chem., Int. Ed.* **2010**, *49*, 2198. (d) Romain, C.; Heinrich, B.; Bellemin-Laponnaz, S.; Dagorne, S. *Chem. Commun.* **2012**, *48*, 2213. (e) Dagorne, S.; Bellemin-Laponnaz, S.; Romain, C. *Organometallics* **2013**, *32*, 2736. (f) Romain, C.; Fliedel, C.; Bellemin-Laponnaz, S.; Dagorne, S. *Organometallics* **2014**, DOI: 10.1021/om5004557.
(25) (a) Yagyu, T.; Oya, S.; Maeda, M.; Jitsukawa, K. *Chem. Lett.* **2006**, *35*, 154. (b) Weinberg, D. R.; Hazari, N.; Labinger, J. A.; Bercaw, J. E. *Organometallics* **2010**, *29*, 89. (c) Boydston, A. J.; Rice, J. D.; Sanderson, M. D.; Dykhno, O. L.; Bielawski, C. W. *Organometallics* **2006**, *25*, 6087. (d) Komiya, N.; Yoshida, A.; Naota, T. *Inorg. Chem. Commun.* **2013**, *27*, 122. (e) Sellmann, D.; Prechtel, W.; Knoch, F.; Moll, M. *Inorg. Chem.* **1993**, *32*, 538.
(26) For an initial synthesis of the protio ligand of **B**, see: Bellemin-Laponnaz, S.; Dagorne, S.; Romain, C.; Steffanut, P. PCT Int. Pat. Appl. WO 2012076140 (A1), 2012.
(27) (a) Chardon, E.; Dahm, G.; Guichard, G.; Bellemin-Laponnaz, S. *Chem. Asian J.* **2013**, *8*, 1232. (b) Chardon, E.; Dahm, G.; Guichard, G.; Bellemin-Laponnaz, S. *Organometallics* **2012**, *31*, 7618.
(28) Crystal data for complex $\mathbf{2_{Pt}}$: $C_{40}H_{49}N_3O_2Pt$, space group $P2_1/c$, a = 5.8864(15) Å, b = 19.331(5) Å, c = 31.025(9) Å, cell volume 3530.4(16) Å^3, Z = 4.

(29) (a) Cao, P.; Cabrera, J.; Padilla, R.; Serra, D.; Rominger, F.; Limbach, M. *Organometallics* **2012**, *31*, 921. (b) Meyer, D.; Zeller, A.; Strassner, T. *J. Organomet. Chem.* **2012**, *701*, 56. (c) Adhikary, S. D.; Bose, D.; Mitra, P.; Saha, K. D.; Bertolasi, V.; Dinda, J. *New J. Chem.* **2012**, *36*, 759. (d) Jahnke, M. C.; Pape, T.; Hahn, F. E. *Z. Naturforsch., B: Chem. Sci.* **2010**, *65*, 341. (e) Schneider, N.; Bellemin-Laponnaz, S.; Wadepohl, H.; Gade, L. H. *Eur. J. Inorg. Chem.* **2008**, 5587. (f) Poyatos, M.; Maisse-François, A.; Bellemin-Laponnaz, S.; Gade, L. H. *Organometallics* **2006**, *25*, 2634.
(30) Nolan, S. P. PCT Int. Pat. Appl. WO 2008036084 (A1), 2008.
(31) Benhamou, L.; Chardon, E.; Lavigne, G.; Bellemin-Laponnaz, S.; César, V. *Chem. Rev.* **2011**, *111*, 2705.
(32) (a) Kong, Y.; Cheng, M.; Ren, H.; Xu, S.; Song, H.; Yang, M.; Liu, B.; Wang, B. *Organometallics* **2011**, *30*, 1677. (b) Waltman, A. W.; Ritter, T.; Grubbs, R. H. *Organometallics* **2006**, *25*, 4238. (c) Li, W.-F.; Sun, H.-M.; Wang, Z.-G.; Chen, M.-Z.; Shen, Q.; Zhang, Y. *J. Organomet. Chem.* **2005**, *690*, 6227.
(33) (a) Perdew, J. P.; Burke, K.; Ernzerhof, M. *Phys. Rev. Lett.* **1996**, *77*, 3865. (b) Perdew, J. P.; Burke, K.; Ernzerhof, M. *Phys. Rev. Lett.* **1997**, *78*, 1396. (c) Adamo, C.; Barone, V. J. *Chem. Phys.* **1999**, *110*, 6158.
(34) Called pbe1pbe in Gaussian09.
(35) van der Ploeg, A. F. M. J.; van Koten, G.; Schitz, J. E. J.; van der Linden, J. G. M. *Inorg. Chim. Acta* **1982**, *58*, 53.
(36) Another possible mode of deactivation in solution could be the decoordination of a phenoxide ligand, particularly in protic solvents. This possibility has been ruled out by conducting VT-NMR experiments. No change in the proton NMR spectra (in methanol) was observed even upon heating (up to 60 °C).
(37) Connick, W. B.; Miskowski, V. M.; Houlding, V. H.; Gray, H. B. *Inorg. Chem.* **2000**, *39*, 2585.
(38) (a) Jude, H.; Bauer, J. A. K.; Connick, W. B. *Inorg. Chem.* **2002**, *41*, 2275. (b) Jude, H.; Bauer, J. A. K.; Connick, W. B. *Inorg. Chem.* **2005**, *44*, 1211.
(39) It should be kept in mind that, upon photoexcitation, energetic solvent stabilization effects on the polar triplet excited state of the complex, which are favored by higher solvent polarity, are not taken into account due to the fact that we are here considering $S_0 \rightarrow T_m$ excitation transitions, rather than $S_0 \leftarrow T_1$ de-excitation processes.
(40) Lewis, F. D.; Miller, A. M.; Salvi, G. D. *Inorg. Chem.* **1995**, *34*, 3173.
(41) Francl, M. M.; Pietro, W. J.; Hehre, W. J.; Binkley, J. S.; Gordon, M. S.; De Frees, D. J.; Pople, J. A. *J. Chem. Phys.* **1982**, *77*, 3654.
(42) (a) Stratmann, R. E.; Scuseria, G. E. *J. Chem. Phys.* **1998**, *109*, 8218. (b) Casida, M. E.; Jamorski, C.; Casida, K. C.; Salahub, D. R. *J. Chem. Phys.* **1998**, *108*, 4439.
(43) Scalmani, G.; Frisch, M. J. *J. Chem. Phys.* **2010**, *132*, 114110.
(44) Frisch, M. J.; Trucks, G. W.; Schlegel, H. B.; Scuseria, G. E.; Robb, M. A.; Cheeseman, J. R.; Montgomery, J. A., Jr.; Vreven, T.; Kudin, K. N.; Burant, J. C.; Millam, J. M.; Iyengar, S. S.; Tomasi, J.; Barone, V.; Mennucci, B.; Cossi, M.; Scalmani, G.; Rega, N.; Petersson, G. A.; Nakatsuji, H.; Hada, M.; Ehara, M.; Toyota, K.; Fukuda, R.; Hasegawa, J.; Ishida, M.; Nakajima, T.; Honda, Y.; Kitao, O.; Nakai, H.; Klene, M.; Li, X.; Knox, J. E.; Hratchian, H. P.; Cross, J. B.; Bakken, V.; Adamo, C.; Jaramillo, J.; Gomperts, R.; Stratmann, R. E.; Yazyev, O.; Austin, A. J.; Cammi, R.; Pomelli, C.; Ochterski, J. W.; Ayala, P. Y.; Morokuma, K.; Voth, G. A.; Salvador, P.; Dannenberg, J. J.; Zakrzewski, V. G.; Dapprich, S.; Daniels, A. D.; Strain, M. C.; Farkas, O.; Malick, D. K.; Rabuck, A. D.; Raghavachari, K.; Foresman, J. B.; Ortiz, J. V.; Cui, Q.; Baboul, A. G.; Clifford, S.; Cioslowski, J.; Stefanov, B. B.; Liu, G.; Liashenko, A.; Piskorz, P.; Komaromi, I.; Martin, R. L.; Fox, D. J.; Keith, T.; Al-Laham, M. A.; Peng, C. Y.; Nanayakkara, A.; Challacombe, M.; Gill, P. M. W.; Johnson, B.; Chen, W.; Wong, M. W.; Gonzalez, C.; Pople, J. A. *Gaussian 09, Revision B.1*; Gaussian, Inc., Wallingford, CT, 2009.